



## Paleoproterozoic Granitoids on Liaodong Peninsula, North China Craton

ZHU Kai<sup>1</sup>, LIU Zhenghong<sup>2,\*</sup>, XU Zhongyuan<sup>2</sup>, LIU Jiexun<sup>2</sup> and WANG Xing'an<sup>3</sup>

<sup>1</sup> College of Geo-exploration Science and Technology, Jilin University, Changchun 130061, China

<sup>2</sup> College of Earth Sciences, Jilin University, Changchun 130061, China

<sup>3</sup> College of Geographical Sciences, Northeast Normal University, Changchun 130024, China

**Abstract:** Paleoproterozoic granitoids are an important constituent of the Jiao–Liao–Ji Belt (JLJB). The spatial-temporal distribution and types of Paleoproterozoic granitoids are closely related to the evolution of the JLJB. In this paper, we review the field occurrence, petrography, geochronology, and geochemistry of Paleoproterozoic granitoids on Liaodong Peninsula, northeast China. The Paleoproterozoic granitoids can be divided into pre-tectonic (~2.15 Ga; peak age=2.18 Ga) and post-tectonic (~1.85 Ga) granitoids. The pre-tectonic granitoids are magnetite and hornblende–biotite monzogranites and granodiorites. Pre-tectonic monzogranites are widespread in the JLJB and have A<sub>2</sub>-type affinities. In contrast, pre-tectonic granodiorites are only present in the Simenzi area and have adakitic affinities. The post-tectonic granitoids consist of porphyritic monzogranite, syenite, diorite, granodiorite, quartz monzonite, monzogranite, and granitic pegmatite, which are adakitic rocks and I-, S-, and A<sub>2</sub>-type granitoids. The assemblage of pre-tectonic A<sub>2</sub>-type granitoids and adakitic rocks indicates the initial tectonic setting of the JLJB was a continental back-arc basin. The assemblage of post-tectonic adakitic rocks and I-, S-, and A<sub>2</sub>-type granitoids indicates a post-collisional setting. The 2.20–2.15 Ga A<sub>2</sub>-type granitoids and adakitic rocks were associated with the initial stage of back-arc extension, and the peak of back-arc extension is inferred from the subsequent (2.15–2.10 Ga) mafic intrusive activity. The ~1.90 Ga adakitic rocks mark the beginning of the post-collisional stage, which was followed by the intrusion of low-temperature S- and I-type granitoids. High- to low-pressure granitoids (S-type) were generated during the peak of post-collisional lithospheric delamination and asthenospheric upwelling. The emplacement of later granitic pegmatites occurred during the waning of the orogeny.

**Key words:** Paleoproterozoic granitoids, pre-tectonic granitoids, post-tectonic granitoids, post-collision, continental back-arc basin, Jiao–Liao–Ji Belt

Citation: Zhu et al., 2019. Paleoproterozoic granitoids on Liaodong Peninsula, North China Craton. *Acta Geologica Sinica (English Edition)*, 93(5): 1377–1396. DOI: 10.1111/1755-6724.14387

### 1 Introduction

The North China Craton (NCC) can be divided into four micro-continental blocks and three Paleoproterozoic mobile belts, based on lithological, structural, metamorphic, and geochronological data (Fig. 1; Zhao et al., 1998, 2005, 2012). The Yinshan and Ordos blocks were amalgamated along the Khondalite Belt at ~1.95 Ga, forming the Western Block (Zhao et al., 2005, 2012; Wan et al., 2006; Xia et al., 2006a, b). The Longgang and Liaonan–Rangnim blocks collided along the Jiao–Liao–Ji Belt (JLJB) at ~1.90 Ga and formed the Eastern Block (Fig. 2). The Trans-North China Orogen resulted from the amalgamation of the Western and Eastern blocks at ~1.85 Ga (Zhao et al., 2001, 2005, 2012).

The JLJB is the most controversial Paleoproterozoic mobile belt in the NCC. It is a NE–SW-trending belt that has experienced a complex tectonic evolution involving multi-stage magmatism, metamorphism, and deformation (Li et al., 1996, 1997, 2005; He and Ye, 1998; Zhao et al., 2012; Liu et al., 2015, 2018; Wang et al., 2015; Xu et al.,

2019). Previous geochronological studies have reported that the JLJB was active from 2.2 to 1.8 Ga (e.g., Zhang and Yang, 1988; Lu, 2004; Lu et al., 2005, 2006; Li and Zhao, 2007; Zhao et al., 2012; Meng et al., 2013, 2017a–c; Li and Chen, 2014, 2016; Liu et al., 2015, 2018; Wang et al., 2015; Li C et al., 2017a; Wang X J et al., 2017; Xu et al., 2019). The evolution of the JLJB can be divided into three stages: (1) the early extensional stage (2.20–2.10 Ga); (2) the basin closure and following collisional stages (2.10–1.90 Ga); and (3) the post-collisional stage (1.90–1.80 Ga) (e.g., Zhang and Yang, 1988; Bai, 1993; Lu, 2004; Zhao et al., 2012; Liu et al., 2015, 2018; Wang et al., 2015; Xu et al., 2019). Although the ~1.9 Ga orogenic event is identified by the high-pressure metamorphic belt on Shandong Peninsula (Liu et al., 2010, 2011a–b, 2012, 2013, 2015), the initial tectonic setting of the JLJB is debated (e.g., Zhang and Yang, 1988; Bai, 1993; Lu et al., 2006; Zhao et al., 2012; Liu et al., 2015, 2018; Wang et al., 2015; Xu et al., 2019). The debate centers on whether the JLJB was a rift (e.g., Zhang and Yang, 1988; Li et al., 2006; Li and Zhao, 2012; Zhao et al., 2012; Wang X P et al., 2017; Liu et al., 2018) or an arc–continent collisional belt (e.g., Bai, 1993; Faure et al., 2004; Wang et al., 2015;

\* Corresponding author. E-mail: zhliu@jlu.edu.cn

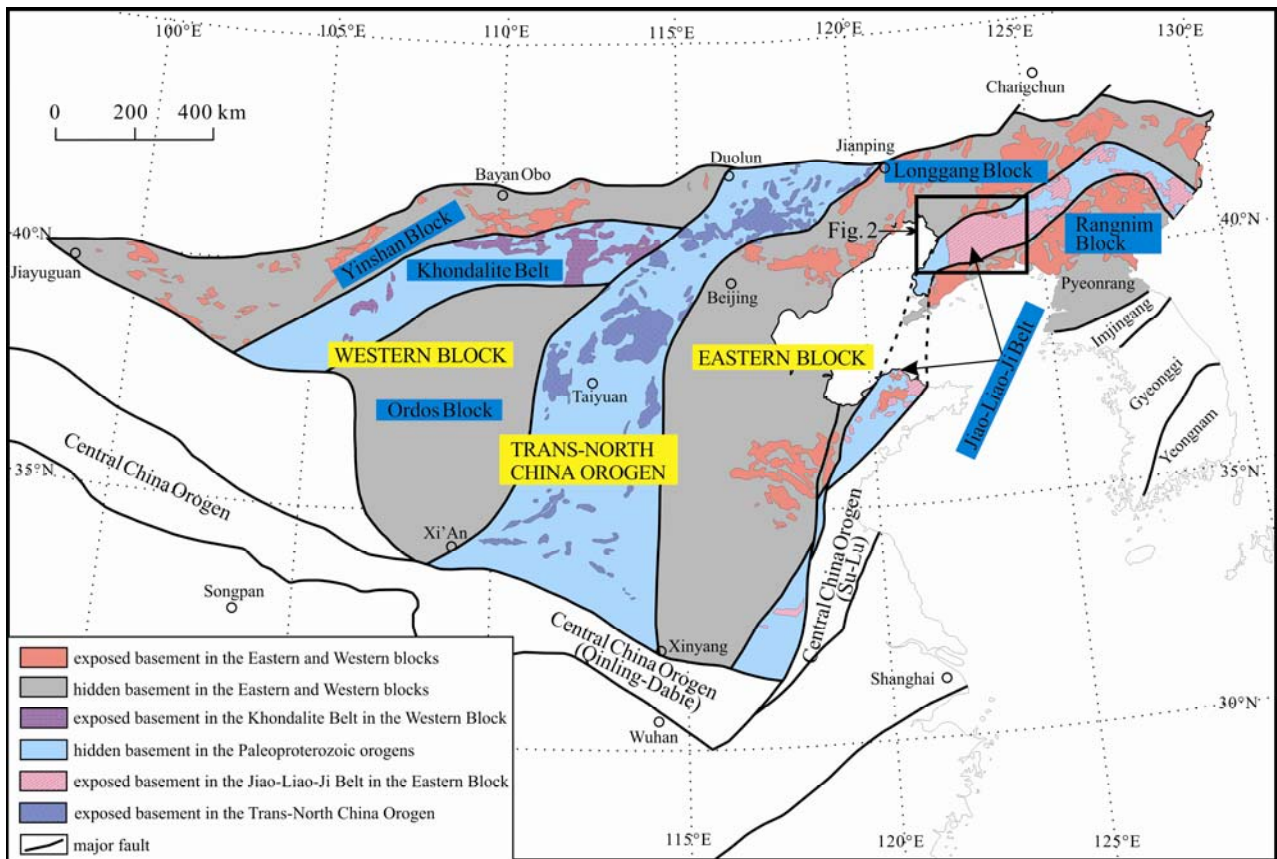


Fig. 1. Tectonic outline of the North China Craton (after Zhao et al., 2005, 2012). The black rectangle shows the location of Fig. 2.

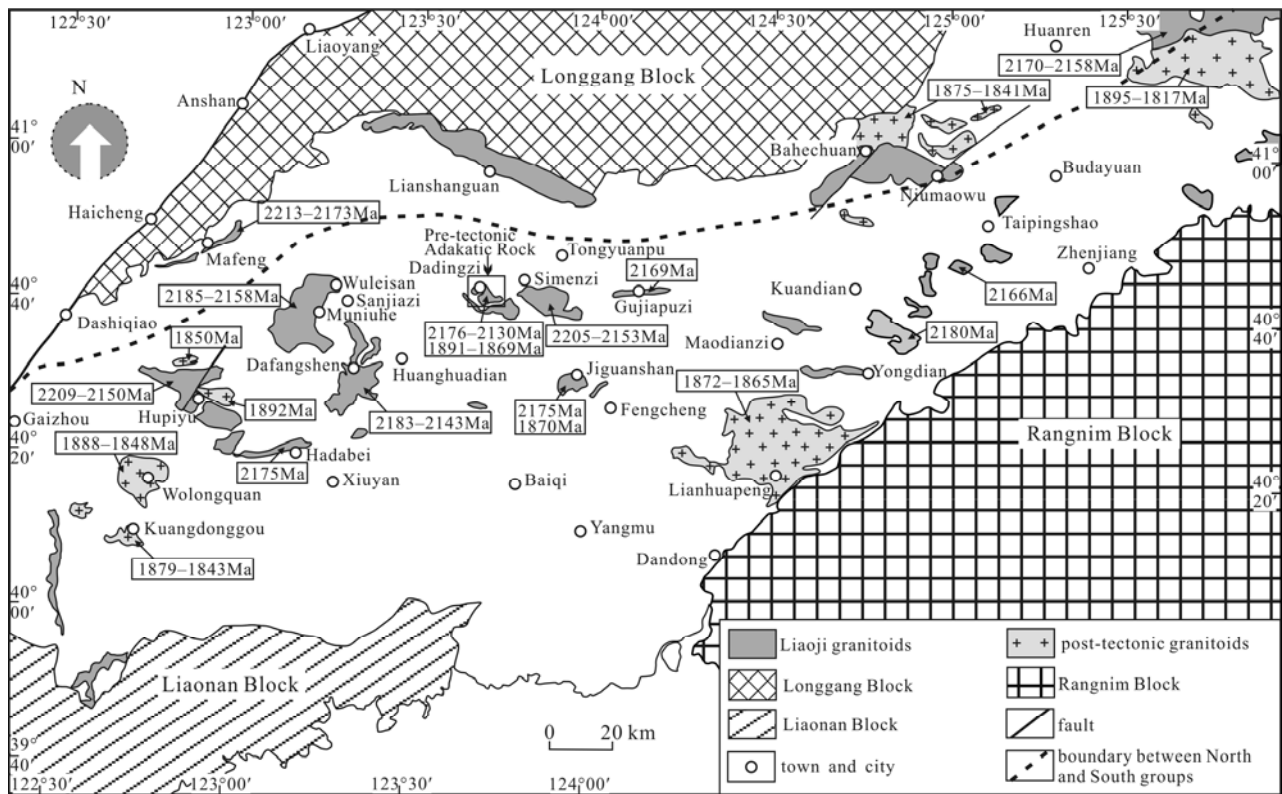


Fig. 2. Map of the Jiao-Liao-Ji Belt showing the distribution of Paleoproterozoic granitoids on Liaodong Peninsula (after Li and Zhao, 2007). The age data and related references in this figure are listed in Table 1.

Li et al., 2015a–b, 2016, 2019; Yuan et al., 2015; Li Z et al., 2017; Wang F et al., 2017; Xu et al., 2019). The presence of widespread pre-tectonic A-type granitoids (e.g., Zhang and Yang, 1988; Hao et al., 2004; Lu et al., 2004a; Li and Zhao, 2007; Yuan et al., 2015), bimodal volcanic rocks (Zhang and Yang, 1988), and the low-pressure and anticlockwise metamorphic  $P$ – $T$ – $t$  paths of Liaohe Group rocks (He and Ye, 1998) indicate an intra-continental rift setting. However, the pre-tectonic A-type granitoids and associated volcanic rocks are depleted in Nb, Ta, and Ti, and have a subduction zone affinity (Meng et al., 2014, 2017a, c; Chen et al., 2016; Li et al., 2016, 2019).

Paleoproterozoic granitoids are an important constituent of the JLJB, and the granitoid types in the JLJB changed as the belt evolved. The pre-tectonic granitoids were once considered to comprise only A-type granitoids and indicate an extensional environment (Zhang and Yang, 1988; Lu et al., 2004a–b; Qin, 2013; Xu et al., 2019). Recently, some ~2.15 Ga adakitic rocks have been identified in the Simenzi area, which provide important evidence for the arc–continent collisional model (Zhu et al., 2019). The ~1.85 Ga granitoids comprise a variety of rock types, indicating complex evolutionary and petrogenetic processes. These Paleoproterozoic granitoids provide important information on the geological evolution of the JLJB. Xu et al. (2019) identified five magmatic flare-ups during the evolution of the JLJB. However, the geological significance of the pre-tectonic adakitic and various post-tectonic granitoids has not been considered. The various types of Paleoproterozoic granitoids on Liaodong Peninsula can provide new insights into the evolution of the JLJB.

In this paper, we review the petrological, geochronological, and geochemical features of the Paleoproterozoic granitoids on Liaodong Peninsula (Fig. 2), and discuss the petrogenesis and geological significance of these granitoids, as well as some outstanding questions regarding their formation.

## 2 Geological Background

The JLJB separates the Eastern Block into the Longgang and Liaonan–Rangnim blocks (Fig. 2). The Longgang Block comprises mainly Archean tonalite–trondhjemite–granodiorite (TTG) rocks and K-rich granitoids, including some 3.8–3.0 Ga complex rocks, 3.3 Ga gneisses, 3.1 Ga trondhjemites, 3.0 Ga monzogranites, 2.5 Ga TTG rocks and monzogranites, and meta-supracrustal rocks (Liu et al., 1992; Song et al., 1996; Wan et al., 1998, 2002, 2005, 2007, 2012a–b, 2013, 2015; Wu et al., 1998; Wu et al., 2008). Although rocks older than 2.6 Ga have not yet been discovered in the Liaonan Block, its ~2.5 Ga plutonic rocks are comparable to those in the Longgang Block, suggesting a similar origin (Lu et al., 2004a; Luo et al., 2008; Zhao et al., 2012; Wang W et al., 2017; Wang M J et al., 2017). The Rangnim Block was considered to be an Archean block similar to the Longgang Block (Li and Zhao, 2007; Luo et al., 2008; Zhao et al., 2012). However, recent studies have revealed that Archean rocks are sporadically distributed in the Longgang Block, and this

block consists mainly of 2.1–1.9 Ga rocks that are similar to those in the JLJB (Zhao et al., 2006; Wu et al., 2016). Therefore, some studies have proposed that the Rangnim Block is a Paleoproterozoic unit like the Liaoji belt rather than an Archean massif (Zhao et al., 2006, 2016; Wu et al., 2007, 2016; Wang et al., 2015).

A series of meta-sedimentary and volcanic successions with associated granitic and mafic intrusions crop out in the JLJB of Liaodong Peninsula (e.g., Zhang and Yang, 1988; Luo et al., 2004, 2008; Meng et al., 2013, 2017a–c; Liu et al., 2015; Wang et al., 2015; Bi et al., 2018; Xu et al., 2019). Based on lithological, structural, metamorphic, and geochronological investigations, the JLJB can be divided into North and South sub-belts along a line that joins the towns of Gaixian–Ximucheng–Taziling–Jiangcaodianzi–Aiyang (Fig. 2). The two sub-belts are in tectonic contact (Wang et al., 2015). The North Sub-belt contains the Laoling, North Liaohe, and Fenzishan groups, and the South Sub-belt comprises the Ji’an, South Liaohe, Jingshan, and Wuhe groups (Liu et al., 2015). Paleoproterozoic granitoids are widespread in the JLJB and can be divided into pre-tectonic (~2.15 Ga; also known as the Liaoji granitoids) and post-tectonic (~1.85 Ga) granitoids (Table 1). A few ~2.0 Ga granitoids are present in the JLJB (Wang P S et al., 2017), but their field occurrence is dike-like rather than large plutons. Most of the post-tectonic granitoids formed at ~1.9 Ga (Ren et al., 2017).

## 3 Field Geology and Petrography

### 3.1 Pre-tectonic granitoids

The pre-tectonic granitoids formed in the early stages of the JLJB, and have a gneissic structure (Fig. 3a–d). They comprise mainly magnetite and hornblende–biotite monzogranitic gneisses, and are K-rich (Zhang and Yang, 1988; Hao et al., 2004; Lu et al., 2004a–b; Li and Zhao, 2007; Ren et al., 2017; Wang et al., 2015). Recently, some granodiorites have been identified in the Simenzi and Muniuhe areas (Fig. 3e–f; Yang et al., 2015a; Song et al., 2016; Zhu et al., 2019). These granodiorites are characterized by a Na-rich geochemistry and complex zircon age compositions (Zhu et al., 2019).

Monzogranitic gneisses are the most common granitic intrusions in the JLJB, whereas the coeval granodiorites are restricted to a few areas (e.g., Simenzi and Muniuhe) (Zhang and Yang, 1988; Li and Zhao, 2007; Yang et al., 2015a; Song et al., 2016; Ren et al., 2017; Zhu et al., 2019). Most of the Liaoji granitoids occupy the cores of WNW–ESE-trending or NW–SE-trending anticlines, which are composed of meta-sedimentary rocks (Zhang and Yang, 1988). Most of the pre-tectonic granitic plutons contain a gneissosity that is parallel to the bedding of the Liaohe Group rocks (Li et al., 1996; Li and Zhao, 2007). These observations are consistent with an emplacement model of uplift bedding–delamination (Li et al., 1996, 1997). Contacts between the Liaoji granitoids and Liaohe Group are mainly tectonic in nature (Liu et al., 2015; Wang et al., 2015), although intrusive contacts are observed in some areas (Liu et al., 2007; Feng et al., 2008; Liu et al., 2015; Wang et al., 2015). Xenoliths of the

**Table 1 Summary of age data for the Paleoproterozoic granitoids (from west to east)**

No.	Pluton	Sample	Lithology	Type	Age (Ma)	Analytical method	Location	References
Pre-tectonic granitoids								
1	Hupiyu	FW01-327	Granitic gneiss	A <sub>2</sub>	2161±12	Zircon (LA-ICP-MS)	Hupiyu Village	Lu et al. (2004a)
		LJ044	Monzogranitic gneiss	A <sub>2</sub>	2150±17	Zircon (SHRIMP)		Li and Zhao (2007)
		NHP01	Monzogranitic gneiss	A <sub>2</sub>	2173±20	Zircon (LA-ICP-MS)		Qin (2013)
		LZ02-1	Granitic gneiss	A <sub>2</sub>	2189±10	Zircon (LA-ICP-MS)		Li and Chen (2014)
		LZ04-1	Granitic gneiss	A <sub>2</sub>	2172±8	Zircon (LA-ICP-MS)		Li and Chen (2014)
		LZ19-1	Granitic gneiss	A <sub>2</sub>	2158±23	Zircon (LA-ICP-MS)		Li and Chen (2014)
		HPX1	Gneissic granite	A <sub>2</sub>	2209±12	Zircon (LA-ICP-MS)		Chen et al. (2016)
		13LJ03	Gneissic granite	A <sub>2</sub>	2119±16	Zircon (LA-ICP-MS)		Ren et al. (2017)
2	Mafeng	NHP-11	Gneissic granite	A <sub>2</sub>	2180±14	Zircon (LA-ICP-MS)	Zhu et al. (2019)	
		LD9822	Granite	A <sub>2</sub>	2173±4	Zircon (SHRIMP)	Wan et al. (2006)	
		LJ056	Monzogranitic gneiss	A <sub>2</sub>	2176±11	Zircon (SHRIMP)	Li and Zhao (2007)	
		LC1	Monzogranitic gneiss	A <sub>2</sub>	2205±6	Zircon (LA-ICP-MS)	Li C et al. (2017a)	
3	Hadabei	LC26	Granitic gneiss	A <sub>2</sub>	2213±6	Zircon (LA-ICP-MS)	Li C et al. (2017a)	
		601SDG1	Monzogranite	A <sub>2</sub>	2181±6	Zircon (CAMECA)	Wang X P et al. (2017)	
4	Muniuhe	HD-2	Granitic gneiss	A <sub>2</sub>	2175±3	Zircon (LA-ICP-MS)	Hadabei Town	Yang et al. (2015a)
5	Dafangshen	D1001-B1	Monzogranite	A <sub>2</sub>	218±29	Zircon (LA-ICP-MS)	Muniuhe Town	Wang P S et al. (2017)
		NMN-5	Monzogranite	A <sub>2</sub>	2158±14	Zircon (LA-ICP-MS)	This study	
		LJ040	Monzogranitic gneiss	A <sub>2</sub>	2143±17	Zircon (SHRIMP)	Li and Zhao (2007)	
		D3208-B1	Monzogranite	A <sub>2</sub>	2183±13	Zircon (LA-ICP-MS)	Dafangshen Town	Wang P S et al. (2017)
6	Dadingzi	D5132-B1	Monzogranite	A <sub>2</sub>	2166±13	Zircon (LA-ICP-MS)	Wang et al. (2017)	
		NXK-1	Monzogranitic gneiss	A <sub>2</sub>	2179±4	Zircon (LA-ICP-MS)	This study	
		TW13	Monzogranite	Adakite	1869±16	Zircon (SHRIMP)	West of the Simenzi Town	Song et al. (2016)
		DTY-8	Granodiorite	Adakite	2173±11	Zircon (LA-ICP-MS)	Zhu et al. (2019)	
		P32TW2-1	Plagiogranite	Adakite	2176±14	Zircon (LA-ICP-MS)	West of the Simenzi Town	Geological Survey Institute of Liaoning Province (2019)
7	Fangjieweizi	719FSG1	Plagiogranite	Adakite	1891±10	Zircon (CAMECA)	Wang X P et al. (2017)	
		DTY-8	Granodiorite	A <sub>2</sub>	2130±24	Zircon (LA-ICP-MS)	West of the Simenzi Town	Zhu et al. (2019)
8	Simenzi	SM-1	Monzogranitic gneiss	A <sub>2</sub>	2205±2	Zircon (LA-ICP-MS)	Simenzi Town	Yang et al. (2015a)
		TW12	Monzogranite	Adakite	2153±16	Zircon (SHRIMP)	Song et al. (2016)	
9	Jiguanshan	LJ035	Monzogranitic gneiss	A <sub>2</sub>	2175±13	Zircon (SHRIMP)	Jiguanshan Town	Li and Zhao (2007)
		LN6	Porphyritic monzogranite	A <sub>2</sub>	1870±7/ 1850±11	Zircon (LA-ICP-MS)	Liu et al. (2017)	
10	Gujiapuzi	T02-1	Syenogranite	A <sub>2</sub>	2169±11	Zircon (SHRIMP)	Gujiapuzi	Song et al. (2016)
11	Yongdian-Budayuan	LJ010	Monzogranitic gneiss	A <sub>2</sub>	2166±14	Zircon (SHRIMP)	Li and Zhao (2007)	
		LC110	Monzogranitic gneiss	A <sub>2</sub>	2178±7	Zircon (LA-ICP-MS)	Li C et al. (2017a)	
		LC126	Monzogranitic gneiss	A <sub>2</sub>	2180±6	Zircon (LA-ICP-MS)	Between the Yongdian and Budayuan towns	Li C et al. (2017a)
		NYD-3	Granitic gneiss	A <sub>2</sub>	2180±5	Zircon (LA-ICP-MS)	Teng et al. (2017)	
		16LN13-1	Monzogranitic gneiss	A <sub>2</sub>	2177 ± 15	Zircon (LA-ICP-MS)	Wang X J et al. (2017)	
12	Qianzhuogou	16LN23-1	Monzogranitic gneiss	A <sub>2</sub>	2177±9	Zircon (LA-ICP-MS)	Wang X J et al. (2017)	
		Lu0007	Syenogranite	A <sub>2</sub>	2164±8	Zircon (LA-ICP-MS)	Lu (2004)	
		Lu1065	Syenogranite	A <sub>2</sub>	2158±13	Zircon (LA-ICP-MS)	Lu (2004)	
		NMY03	Monzogranitic gneiss	A <sub>2</sub>	2168±14	Zircon (LA-ICP-MS)	East of the Huanren County	Qin (2013)
13	Kuangdonggou	NQZ01	Monzogranitic gneiss	A <sub>2</sub>	2170±11	Zircon (LA-ICP-MS)	Qin (2013)	
		FW01-31	Syenite	A <sub>2</sub>	1843±23	Zircon (LA-ICP-MS)	Lu et al. (2004a)	
		03JH079	Syenite	A <sub>2</sub>	1879±11	Zircon (LA-ICP-MS)	Kuangdonggou Town	Yang et al. (2007)
		03JH080	Syenite	A <sub>2</sub>	1872±14	Zircon (LA-ICP-MS)	Yang et al. (2007)	
		03JH082	Diorite	A <sub>2</sub>	1870±18	Zircon (LA-ICP-MS)	Yang et al. (2007)	
14	Wolongquan	FW02-62	Porphyritic monzogranite	S	1848±10	Zircon (LA-ICP-MS)	Wolongquan Town	Lu et al. (2004a)
		RZ10	Porphyritic monzogranite	S	1888.4±5.3	Zircon (LA-ICP-MS)	Wolongquan Town	Liu W B et al. (2018)
15	Nantaizi	11LJ65	Quartz monzonite	I	1850±11	Zircon (LA-ICP-MS)	North of the Hupiyu pluton	Ren et al. (2017)
16	Housongshugou	13LJ11	Granodiorite	Adakite	1892±16	Zircon (LA-ICP-MS)	West of the Hupiyu pluton	Ren et al. (2017)

Continued Table 1

No.	Pluton	Sample	Lithology	Type	Age (Ma)	Analytical method	Location	References
17	Helan	10JLL13	Granitic pegmatite		1875±10	Zircon (LA-ICP-MS)	Helan Town	Wang et al. (2011)
18	Wuleishan	TW11	Porphyritic granite	Adakite	1835 ± 9	Zircon (SHRIMP)	North of the Muniuhe Town	Song et al. (2016)
19	Sanjiazi	16KD54-2	Granitic pegmatite		1876±11	Zircon (LA-ICP-MS)	Around the Sanjiazi Town	Yang et al. (2017)
		16KD66-1	Granitic pegmatite		1802±15	Zircon (LA-ICP-MS)		Yang et al. (2017)
		16KD80-2	Granitic pegmatite		1740±8	Zircon (LA-ICP-MS)		Yang et al. (2017)
		16SJZ07-8	Granitic pegmatite		1871±7	Zircon (LA-ICP-MS)		Yang et al. (2017)
20	Huanghuadian	D1032-B1	Granodiorite	Adakite	1995±18	Zircon (LA-ICP-MS)	Huanghuadian Town	Wang P S et al. (2017)
		D5002-B1	Granodiorite	Adakite	1995±13	Zircon (LA-ICP-MS)		Wang P S et al. (2017)
21	Jiuliancheng	LN3	Porphyritic monzogranite	S	1872±8/1851±12	Zircon (LA-ICP-MS)	Northern of Dandong City	Liu et al. (2017)
		LN4	Porphyritic monzogranite	S	1865±6/1849±8	Zircon (LA-ICP-MS)		Liu et al. (2017)
22	Kuandian	16KD05-4	Granitic pegmatite		1842±13	Zircon (LA-ICP-MS)	Yongdian-Taipingshao towns	Yang et al. (2017)
		16KD06-1	Granitic pegmatite		1864±8	Zircon (LA-ICP-MS)		Yang et al. (2017)
23	Bahechuan	Lu010	Porphyritic monzogranite	S	1841±12	Zircon (SHRIMP)	Bahechuan Town	Lu et al. (2005)
		LJ006	Porphyritic monzogranite	S	1875±10	Zircon (SHRIMP)		Li and Zhao (2007)
		LN5	Porphyritic monzogranite	S	1864±8/1844±9	Zircon (LA-ICP-MS)		Liu et al. (2017)
24	Zhenjiang-Yulin	LN1	Porphyritic monzogranite	S	1867±10/1842±12	Zircon (LA-ICP-MS)	Zhenjiang-Yulin towns	Liu et al. (2017)
		LN2	Porphyritic monzogranite	S	1866±6/1846±13	Zircon (LA-ICP-MS)		Liu et al. (2017)
25	Shuangcha	92015	Porphyritic monzogranite	S	1872±11	Zircon (SHRIMP)	East of Huanren County	Lu et al. (2005)
		12082	Porphyritic monzogranite	S	1817±18	Zircon (SHRIMP)		Lu et al. (2005)
		LJ005	Porphyritic monzogranite	S	1856±31	Zircon (SHRIMP)		Li and Zhao (2007)
		NSC01	Porphyritic monzogranite	S	1877±15	Zircon (LA-ICP-MS)	East of Huanren County	Qin (2013)
		SC-1	Porphyritic monzogranite	S	1895±2	Zircon (LA-ICP-MS)		Yang et al. (2015b)
		JN7	Porphyritic granite	S	1871±7/1850±12	Zircon (LA-ICP-MS)		Liu et al. (2017)
26	Longquan	JN8	Porphyritic granite	S	1872±7/1850±13	Zircon (LA-ICP-MS)	Longquan Town	Liu et al. (2017)
		JN6	Porphyritic granite	S	1865±7/1849 ± 9	Zircon (LA-ICP-MS)		Liu et al. (2017)
27	Qinghe	12072	Quartz diorite	I	1872±11	Zircon (SHRIMP)	Qinghe Town	Lu et al. (2005)

Liaohe Group are present in some pre-tectonic plutons (e.g., Lieryu Formation xenoliths in the Simenzi pluton), suggesting an intrusive contact between such plutons and the lower Liaohe Group (Zhu et al., 2019). Some mafic dikes (~2.15 Ga) were intruded into pre-tectonic granitic plutons (Yang et al., 2015a), and the dikes and granitic plutons were intruded by later granites and granitic pegmatites (Fig. 3g–h).

Compared with the monzogranitic gneisses, the pre-tectonic granodiorites display weak or no gneissosity (Fig. 3e–f). No contacts have been observed between the pre-tectonic granodiorites and lower Liaohe Group (e.g., Lieryu and Gaojiayu formations). A faulted contact between the Gaixian Formation and granodiorites can be observed in the Simenzi area (Fig. 4).

### 3.2 Post-tectonic granitoids

It has become increasingly recognized that post-tectonic granitoids are also widespread in the JLJB (Zhang and Yang, 1988; Lu, 2004; Lu et al., 2005; Qin, 2013; Song et al., 2016; Liu et al., 2017). The post-tectonic granitoids in the JLJB comprise a series of ~1.85 Ga rocks, including the Housongshugou granodiorite, Nantaizi quartz monzonite, Kanzi monzogranite, Kuangdonggou syenite and diorite, widespread porphyritic monzogranite, and granitic pegmatites (Fig. 5; Ge et al., 1991; Lu, 2004; Lu et al., 2004a, 2005; Li and Zhao, 2007; Yang et al., 2007; Wang et al., 2011; Qin, 2013; Yang et al., 2015b; Song et al., 2016; Liu et al., 2017; Ren et al., 2017; Wang P S et al., 2017; Yang et al., 2017). Most of the post-tectonic plutons do not display a gneissosity (Fig. 5c–h), although some have a weak gneissosity (Fig. 5c–h). The post-tectonic granitoids intrude the Liaohe Group and pre-tectonic plutons (Ren et al., 2017; Yang et al., 2017), and

xenoliths of the upper Liaohe Group (e.g., Dashiqiao and Gaixian formations) can be observed in the plutons (Fig. 5i).

## 4 Geochemistry and Magma Sources

In addition to our unpublished data, other data for the granitoids were collated from previous studies (Lu, 2004; Yang et al., 2007; Qin, 2013; Yang et al., 2015a; Song et al., 2016; Liu et al., 2017; Ren et al., 2017; Teng et al., 2017; Wang P S et al., 2017; Liu W B et al., 2018; Zhu et al., 2019), which includes data for 79 pre-tectonic and 43 post-tectonic granitoids. Some plutons have not been analyzed (e.g., Kanzi pluton) and are not discussed further.

### 4.1 Major and trace elements

#### 4.1.1 Pre-tectonic granitoids

SiO<sub>2</sub> contents of the Liaoji granitoids range from 63 to 78 wt%. K<sub>2</sub>O, Na<sub>2</sub>O, CaO, Fe<sub>2</sub>O<sub>3</sub><sup>T</sup>, and Al<sub>2</sub>O<sub>3</sub> contents range from 0.6 to 7.1, 2.2 to 6.2, 0.08 to 3.16, 0.6 to 7.6, and 10.6 to 17.1 wt%, respectively. A/CNK ratios vary from 0.88 to 1.27 (Fig. 6a). In a Na<sub>2</sub>O+K<sub>2</sub>O vs. SiO<sub>2</sub> plot, data for nearly all the Liaoji granitoids plot in the granite field (Fig. 7a). Based on K<sub>2</sub>O and Na<sub>2</sub>O contents, the Liaoji granitoids can be divided into K-rich [ $\omega(K_2O) > \omega(Na_2O)$ ] and Na-rich [ $\omega(Na_2O) > \omega(K_2O)$ ] groups. Most K-rich Liaoji granitoids belong to the shoshonite or high-K calc-alkaline series, whereas the Na-rich granitoids belong to the high-K calc-alkaline, calc-alkaline, or tholeiite series (Fig. 7b).

Based on total rare earth element (TREE) contents, the Liaoji granitoids can be divided into high- and low-TREE groups (Fig. 8a). The low-TREE group comprises some of the Na-rich granitoids, and the high-TREE group



Fig. 3. Photographs of the Liaoji granitoids.

(a–b) Hupiyu granitic gneiss; (c) Simenzi monzogranitic gneiss; (d) Mafeng monzogranitic gneiss; (e) Qianzhuogou monzogranitic gneiss; (f) Dadingzi granodiorite (weak gneissosity); (g) Fangjiaweizi granodiorite (no gneissosity); (h) Hupiyu pluton intruded by mafic and granitic dikes, and (i) mafic dike intruded by granitic pegmatite in the Hupiyu pluton.

comprises all the K-rich and remaining Na-rich granitoids. The Na-rich granitoids have slightly more negative Eu anomalies than the K-rich granitoids. In a primitive-mantle-normalized trace element diagram, data for high-TREE samples exhibit enrichments in Ba, K, Th, and Nd. In contrast, they are depleted in Sr, Nb, P, and Ti (Fig. 8b). The low-TREE samples are enriched in Cs, K, and Sr, and depleted in Th, Nb, and Ti (Fig. 8b). The difference in Sr contents between the high- and low-TREE groups is particularly evident. Thus, the samples can be divided into high-Sr (277–992 ppm) and low-Sr (9.3–150.5 ppm) groups on the basis of Sr contents. In general, the Sr content is related to the pressure of the original magma source (Zhang et al., 2006). Therefore, a classification based on Sr content is more reasonable than that based on  $K_2O$  and  $Na_2O$  contents. Sr and Yb contents indicate that the low-TREE group comprises high-Sr–low-Yb granitoids, whereas the high-TREE group comprises low-Sr–high-Yb granitoids.

#### 4.1.2 Post-tectonic granitoids

$SiO_2$  contents of the post-tectonic granitoids vary from 53 to 76 wt%.  $K_2O$  and  $Na_2O$  contents range from 3.0 to

8.5 wt% and 1.8 to 6.6 wt%, respectively, and  $Fe_2O_3^T$  and  $Al_2O_3$  contents vary from 0.5 to 9.1 wt% and 12.7 to 19.6 wt%, respectively. A/CNK ratios of the post-tectonic granitoids are 0.76 to 1.32 (Fig. 6b). In a TAS (total alkalis–silica) classification diagram, data for Kuangdonggou and Nantaizi samples plot in the syenite and syenodiorite fields, and they are alkaline rocks (Fig. 7c). The other post-tectonic granitoids are subalkaline/tholeiitic rocks that plot in the granite and granodiorite fields (Fig. 7c). Most of the pre-tectonic granitoids belong to the shoshonite or high-K calc-alkaline series, but a few are calc-alkaline (Fig. 7d).

The post-tectonic granitoids can also be divided into high- and low-TREE groups (Fig. 8c), which are consistent with the K-rich (porphyritic monzogranite, syenite, and diorite) and Na-rich (Housongshugou granodiorite and Nantaizi quartz monzonite) groups, respectively. The post-tectonic K-rich samples are enriched in Th, U, K, and Nd, and depleted in Nb, P, and Ti (Fig. 8d). The post-tectonic Na-rich samples are enriched in K, Ba, and Zr, and depleted in Nb, P, and Ti (Fig. 8d). Compared with the pre-tectonic granitoids, the post-tectonic granitoids have more complex geochemical

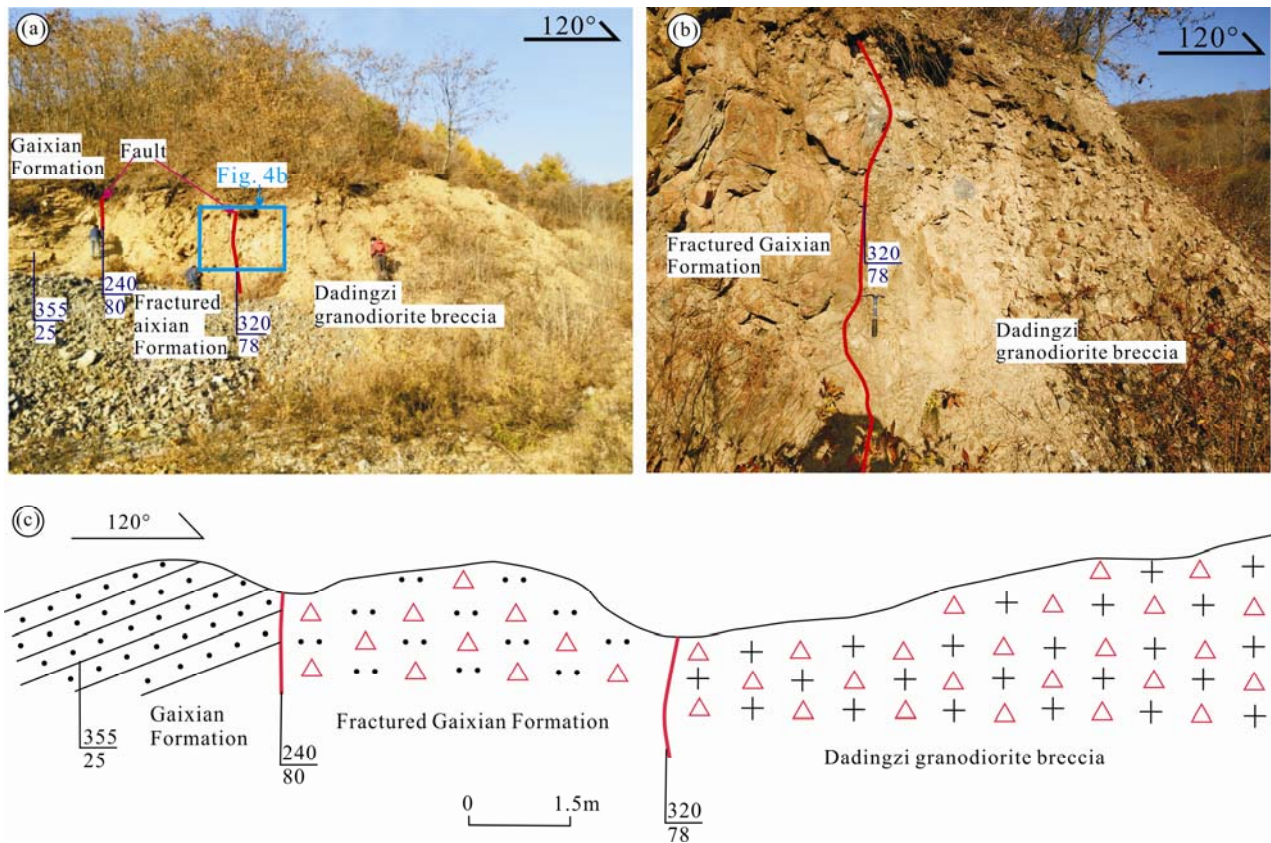


Fig. 4. Photograph and cross-section showing the contact between the Gaixian Formation and Dadingzi pluton (after Zhu et al., 2019).

(a) Faulted contact between the Gaixian Formation and Dadingzi pluton; (b) Contact zone detail; (c) Cross-section of the outcrop shown in (a).

compositions. As such, a classification based on Sr and Yb contents was used for these post-tectonic granitoids (Table 2). Post-tectonic granitoids include low-Sr–high-Yb (all porphyritic monzogranites, except the Wolongquan porphyritic monzogranites), low-Sr–low-Yb (Nantaizi quartz monzonite and four Wolongquan porphyritic monzogranites), high-Sr–high-Yb (Kuangdonggou diorite and two Wolongquan porphyritic monzogranites), and high-Sr–low-Yb types (Housongshugou granodiorite and Kuangdonggou syenite). The two high-Sr–high-Yb Wolongquan samples have a different geochemical

composition from the other four samples (Fig. 8c–d), indicating they may originate from an unknown pluton. The two anomalous samples are not considered further.

## 4.2 Genetic type

### 4.2.1 Pre-tectonic granitoids

In geochemical discrimination diagrams, data for the low-Sr granitoids plot in the field of A-type granitoids (Fig. 9a–b), and the high-Sr samples plot in the I- and S-type fields. In addition, the low-Sr granitoids have high  $\text{FeO}^{\text{T}}$  (>1 wt%), Zr+Nb+Ce+Y (>350 ppm) and magma

**Table 2 Classification of the post-tectonic granitoids on the basis of Sr and Yb contents**

No	Pluton	lithology	number of samples	Sr (ppm)	average	Yb (ppm)	average	classification	references
1	Shuangcha		11						
2	Zhenjiang-Yulin		2						
3	Jiuliancheng	Porphyritic monzogranite	2	45–314	117	1.23–3.55	2.51	Low-Sr–high-Yb	Lu et al. (2006); Liu et al. (2017)
4	Bahechuan		1						
5	Jiguanshan		1						
6	Longquan		1						
7	Wolongquan	Porphyritic monzogranite	4	78.9–361	175	1.52–2.25	1.82	Low-Sr–low-Yb	Liu et al. (2018b)
		Porphyritic monzogranite	2	752–811	782	3.85–4.06	4.00	High-Sr–high-Yb	Liu et al. (2018b)
		syenite	3	665–766	704	1.61–2.20	1.83	High-Sr–low-Yb	Yang et al. (2007)
8	Kuangdonggou	diorite	3	1271–1339	1308	3.44–3.63	3.52	High-Sr–high-Yb	Yang et al. (2007)
9	Housongshugou	Granodiorite	5	287–348	319	0.12–0.24	0.17	High-Sr–low-Yb	Ren et al. (2017)
10	Nantaizi	Quartz monzonite	3	22.1–58.6	34.7	0.38–0.67	0.52	Low-Sr–low-Yb	Ren et al. (2017)



Fig. 5. Photographs of the post-tectonic granitoids. (a–b) Housongshugou granodiorite; (c) Shuangcha porphyritic monzogranite; (d) garnet-bearing granite (Qinghe Town); (e) Kuangdonggou syenite; (f) Wolongquan porphyritic monzogranite; (g) Kanzi monzogranite; (h) tourmaline-bearing granitic pegmatites, and (i) Wolongquan pluton intruding the Gaixian Formation. Grt = garnet; Tur = tourmaline.

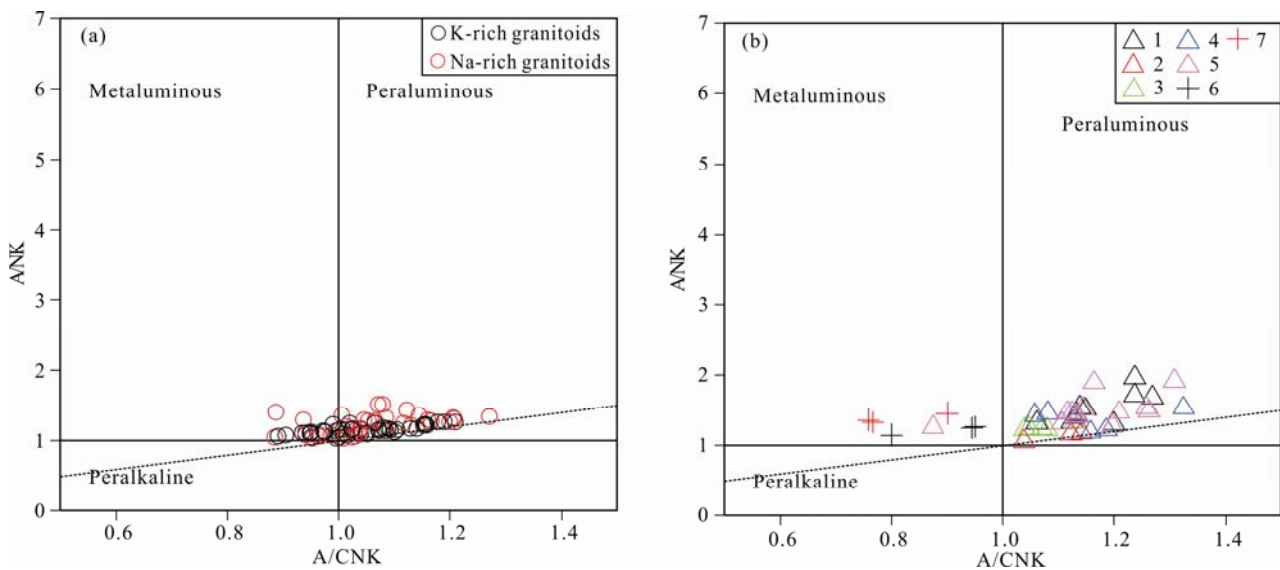


Fig. 6. Aluminous index diagrams for the Paleoproterozoic granitoids. 1 = Shuangcha porphyritic monzogranite; 2 = Nantaizi quartz monzonite; 3 = Housongshugou granodiorite; 4 = Wolongquan porphyritic monzogranite; 5 = porphyritic monzogranite from Liu et al. (2017); 6 = Kuangdonggou syenite; 7 = Kuangdonggou diorite.

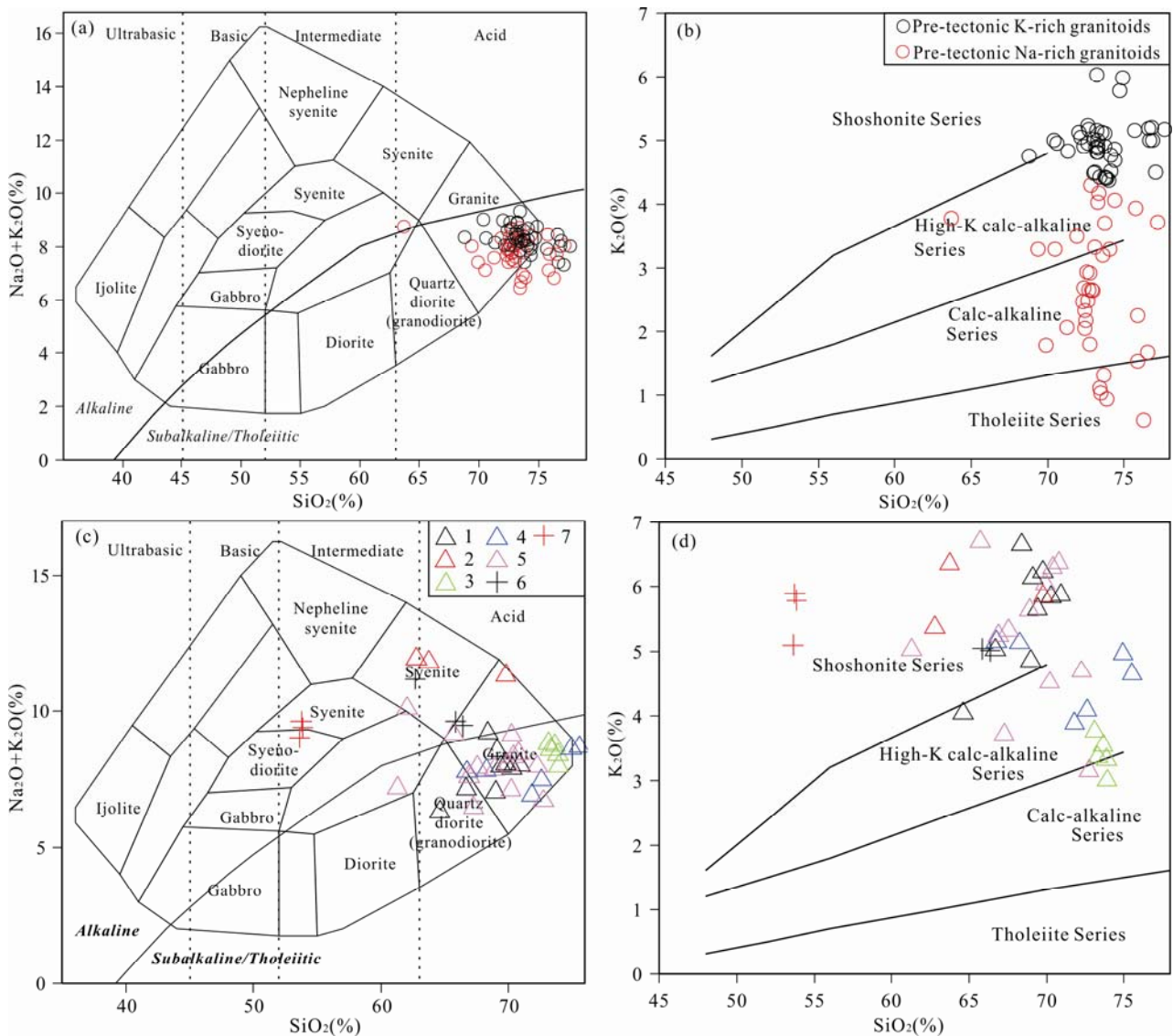


Fig. 7. (a, c) Total alkalis–silica and (b, d)  $\text{SiO}_2$  vs.  $\text{K}_2\text{O}$  classification diagrams for the Paleoproterozoic granitoids.

1 = Shuangcha porphyritic monzogranite; 2 = Nantaizi quartz monzonite; 3 = Housongshugou granodiorite; 4 = Wolongquan porphyritic monzogranite; 5 = porphyritic monzogranite from Liu et al. (2017); 6 = Kuangdonggou syenite; 7 = Kuangdonggou diorite.

temperatures (850–890°C), providing further evidence for their A-type affinities (Wang et al., 2000; Whalen et al., 1987; Eby, 1990; Wu et al., 2007a). The high Sr/Y (70.7–381.5) and low  $\text{P}_2\text{O}_5$  (0.01–0.07 wt%), TREE (15.19–33.14 ppm) contents and magma temperatures (727–738°C) suggest that the high-Sr group are I-type granitoids (Fig. 10a), and have an affinity with adakitic rocks (Fig. 10c).

#### 4.1.2 Post-tectonic granitoids

Data for the Nantaizi, Wolongquan, and Kuangdonggou plutons plot in the A-type field in geochemical discrimination diagrams (Fig. 9c–d). A-type granites are characterized by high  $\text{Zr}+\text{Nb}+\text{Ce}+\text{Y}$  (>350 ppm). However,  $\text{Zr}+\text{Nb}+\text{Ce}+\text{Y}$  contents of the Nantaizi and Wolongquan samples range from 57.2 to 267.5 ppm. Hence, these are high-alkali I- or S-type rather than A-type granitoids. There is negative correlation between  $\text{SiO}_2$  and

$\text{P}_2\text{O}_5$  contents in I-type granitoids, whereas  $\text{SiO}_2$  content has positive correlation with  $\text{P}_2\text{O}_5$  content in S-type granitoids (Li et al., 2007). In a  $\text{SiO}_2$  vs.  $\text{P}_2\text{O}_5$  diagram, the Nantaizi and Wolongquan samples are identified as I- and S-type granitoids, respectively (Fig. 10b). The Kuangdonggou samples are enriched in alkalis and Zr–Y, have high Ga/Al ratios and marked negative Eu anomalies, and display A-type affinities. However, their high Sr (>400 ppm) and low  $\text{SiO}_2$  (<70 wt%) contents suggest they are also different from typical A-type granitoids (Zhang Q et al., 2012). The Housongshugou granodiorites have high Sr/Y and plot in the adakite field in a Sr/Y vs. Y diagram (Fig. 10d). Most of the widespread porphyritic monzogranites contain aluminous primary phases (e.g., muscovite, cordierite, and garnet), and have high A/CNK (>1.1) and  $\text{K}_2\text{O}/\text{Na}_2\text{O}$  ratios, reflecting an S-type affinity (Lu et al., 2005; Liu et al., 2017). Liu et al. (2017) considered these porphyritic monzogranites to be I-type

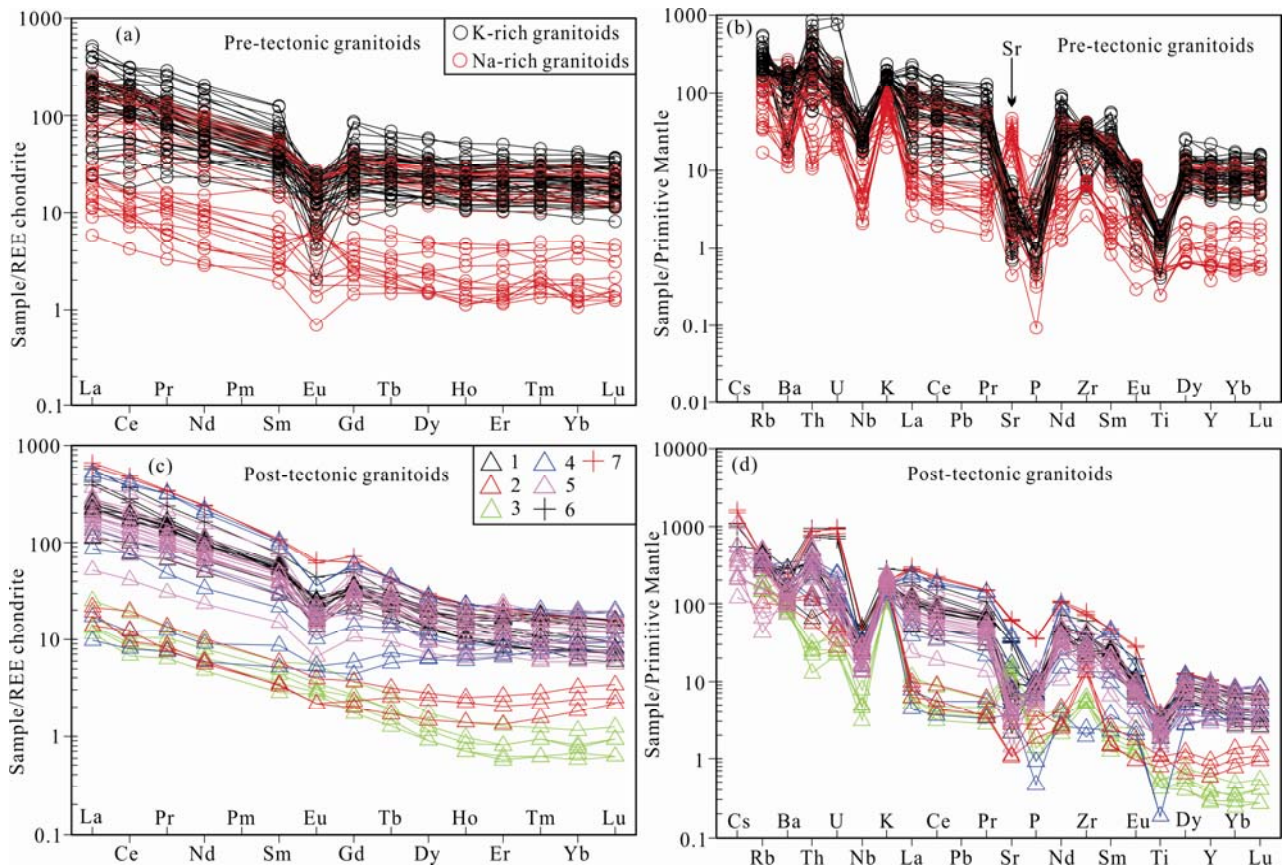


Fig. 8. (a, c) Chondrite-normalized REE patterns (normalization values from Boynton, 1984) and (b, d) primitive-mantle-normalized trace element diagrams for the Paleoproterozoic granitoids (normalization values from Sun and McDonough, 1989). 1 = Shuangcha porphyritic monzogranite; 2 = Nantaizi quartz monzonite; 3 = Housongshugou granodiorite; 4 = Wolongquan porphyritic monzogranite; 5 = porphyritic monzogranite from Liu et al. (2017); 6 = Kuangdonggou syenite; 7 = Kuangdonggou diorite.

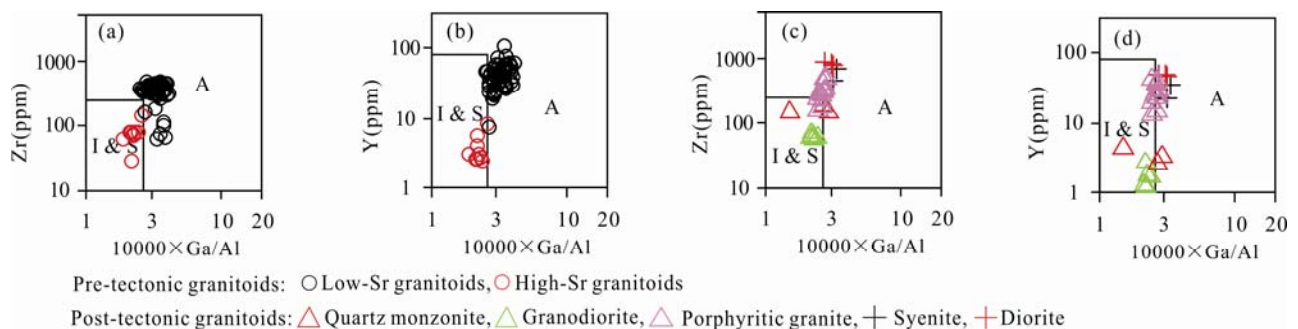


Fig. 9. Geochemical discrimination diagrams for the Paleoproterozoic granitoids (after Whalen et al., 1987). Due to a lack of Ga data, the Wolongquan samples are not shown in this figure.

granitoids based on their high Zr-saturation temperatures (790–908°C) and absence of inherited zircons. Sylvester (1998) suggested that hot (>875°C) strongly peraluminous granites can form in a post-collisional setting and are generated by mantle-derived heating after lithospheric delamination. Cordierite is diagnostic for identifying S-type granitoids (Wu et al., 2007), and is present in the Shuangcha pluton (Lu et al., 2005). Although most of the porphyritic monzogranite plutons lack cordierite, they have similar geochemical compositions as the Shuangcha granitoids (Fig. 8c–d), suggesting a similar petrogenesis.

In addition, most of the data for the porphyritic monzogranites are consistent with the evolutionary trend of S-type granitoids in a  $\text{SiO}_2$  vs.  $\text{P}_2\text{O}_5$  diagram (Fig. 9b).  $\text{CaO}/\text{Na}_2\text{O}$  and  $\text{Al}_2\text{O}_3/\text{TiO}_2$  ratios indicate the Wolongquan porphyritic monzogranites ( $\text{CaO}/\text{Na}_2\text{O}=0.04$ – $0.40$ ;  $\text{Al}_2\text{O}_3/\text{TiO}_2=41.4$ – $347.5$ ) are pelite-derived, low-temperature S-type granitoids, whereas the other samples ( $\text{CaO}/\text{Na}_2\text{O}=0.12$ – $1.15$ ;  $\text{Al}_2\text{O}_3/\text{TiO}_2=16.3$ – $46.8$ ) are psammite-derived, high-temperature S-type granitoids (Sylvester, 1998). Therefore, all the porphyritic monzogranites are S-type. In summary, the post-tectonic

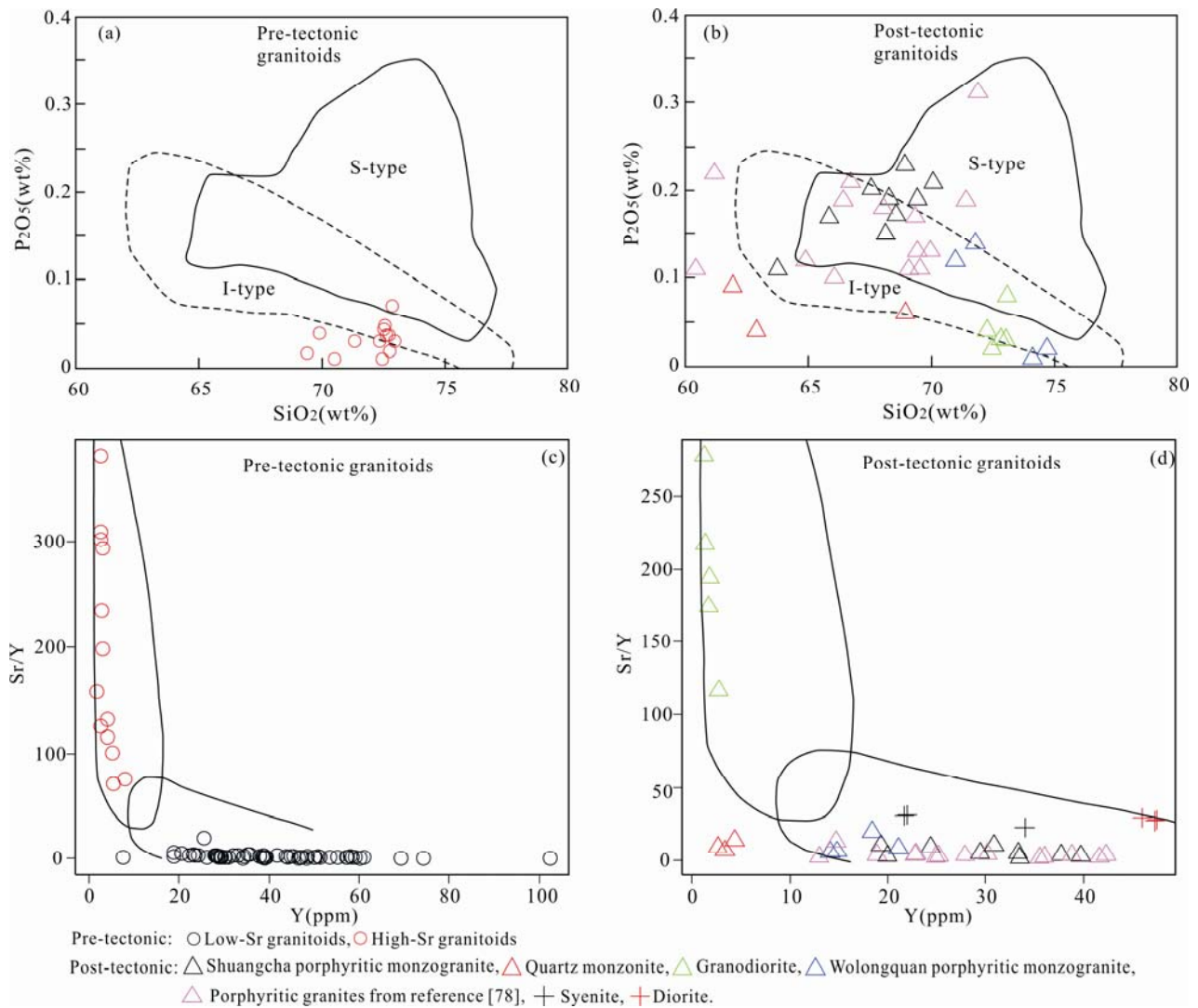


Fig. 10. (a–b)  $P_2O_5$  vs.  $SiO_2$  (after Chappell, 1999) and (c–d)  $Sr/Y$  vs.  $Y$  (after Defant and Drummond, 1990) diagrams for the Paleoproterozoic granitoids.

granitoids include adakitic (Housongshugou granodiorite), A-type (Kuangdonggou syenite and diorite), S-type (porphyritic monzogranite), and I-type (Nantaizi quartz monzonite) rocks.

### 4.3 Magma sources

#### 4.3.1 Pre-tectonic granitoids

The pre-tectonic A-type granitoids in the JLJB are peraluminous, and most likely derived by partial melting of felsic crust, with plagioclase and orthopyroxene being the main residual source minerals (King et al., 1997; Patino Douce, 1997; Zhang et al., 2006). Low  $Sr/Y$  ratios imply that the pre-tectonic A-type granitoids formed in a low-pressure environment (Zhang et al., 2006). The pre-tectonic A-type granitoids show wide range in Hf ( $\epsilon_{Hf}(t) = -1.77$  to  $7.9$ ,  $T_{DM}^C = 3.1$ – $2.3$  Ga) and Nd ( $\epsilon_{Nd}(t) = -8.63$ – $3.03$  and  $T_{DM2} = 3.3$ – $2.4$  Ga) isotope compositions (Song et al., 2016; Yang et al., 2016; Zhu et al., 2019; Hao et al., 2004; Yang et al., 2015a; Li C et al., 2017b; Wang X P et al., 2017). Most of  $T_{DM}^C$  and  $T_{DM2}$  ages range from 2.8 to

2.5 Ga, and few of them are  $\sim 3.0$  and  $\sim 2.3$  Ga (Song et al., 2016; Zhu et al., 2019), reflecting that they were mainly derived from partial melting of Archean crust. The pre-tectonic adakitic granitoids have high  $Al_2O_3$  and Sr contents, significant heavy REE depletion, and small negative Eu anomalies. These features suggest they were derived from thickened crust, and that eclogite or amphibolite was the residual lithology (Ge et al., 2002; Li and Li, 2003; Zhang et al., 2006). The pre-tectonic adakitic granitoids have  $\epsilon_{Hf}(t)$  values of  $-13.04$  to  $+6.72$  and  $T_{DM2}$  of these zircons vary from 3.5 to 2.3 Ga (Zhu et al., 2019). Most  $T_{DM2}$  ages range from 2.9 to 2.6 Ga, suggesting that the adakitic rocks were mainly derived from partial melting of Archean igneous rocks (Zhu et al., 2019). Although both pre-tectonic A-type and adakitic granitoids were mainly derived from partial melting of Archean crust, the  $\sim 2.3$  Ga  $T_{DM}^C/T_{DM2}$  ages and considerable variation in Hf and Nd isotope compositions indicate the existence of juvenile materials (or depleted mantle) in their magma sources.

### 4.3.2 Post-tectonic granitoids

Compared with I-type granitoids, S-type granitoids are lower in Na, Ca, Sr, and  $\text{Fe}^{3+}/\text{Fe}^{2+}$ , and higher in Cr and Ni. Therefore, S-type granitoids have high A/CNK ratios and contain Al-rich minerals. Based on these differences, Chappell and White (1992, 2001) proposed that I- and S-type granitoids are derived by partial melting of intracrustal igneous and supracrustal sedimentary rocks, respectively. The porphyritic granitoids mostly have  $\epsilon\text{Hf}(t)$  and  $T_{\text{DM}}^{\text{C}}$  of  $-5.42$  to  $3.50$  and  $2.9$ – $2.3$  Ga (Yang et al., 2015b; Liu et al., 2017), and  $\epsilon\text{Nd}(t)$  and  $T_{\text{DM}}^{\text{C}}$  of  $-5.02$  to  $-0.74$  and  $2.8$ – $2.4$  Ga (Hao et al., 2004; Yang et al., 2007; Yang et al., 2015b; Wang X P et al., 2017). Their Hf and Nd isotope compositions are similar to those of pre-tectonic granitoids, which is consistent with the fact that pre-tectonic igneous rocks are main provenance of sedimentary rock in the JLJB. Hence, the porphyritic monzogranites were derived by partial melting of sedimentary rocks, whereas the Housongshugou and Nantaizi plutons were derived by partial melting of igneous rocks. Low-silica ( $\text{SiO}_2 < 50$  wt%) syenites were derived from an enriched mantle source (Yang et al., 2005), whereas the high-silica syenites ( $\text{SiO}_2 > 50$  wt%) may be the result of mixing of mantle- and crust-derived magmas (Yang et al., 2007). The Kuangdonggou syenites have high  $\text{SiO}_2$  contents (62.71–66.39 wt%), reflecting derivation by mixing of mantle- and crust-derived magmas (Yang et al., 2007). The similar trace element and Nd isotope ( $\epsilon\text{Nd}(t)$  values of  $-2.3$  to  $-1.5$  for syenite and  $-2.3$  to  $-1.9$  for diorite) of the Kuangdonggou syenite and diorite indicate a similar origin. Hf isotopic model ages of the Kuangdonggou granitoids range from 2.5 to 2.4 Ga, which are younger than the basement of the Eastern Block of the NCC (Yang et al., 2007). In addition, the Kuangdonggou syenites and associated diorites have similar crystallization ages, but have different Hf isotope ratios. These features indicate that the syenites and diorites resulted from mixing of different proportions of mantle- and crust-derived magmas (Yang et al., 2007).

The post-tectonic syenites have high-Sr–low-Yb contents and low Sr/Yb ratios. It is a matter of debate as to whether Sr and Yb contents of syenites are related to the depth of the magma source (Sylvester, 1998; Zhang et al., 2006). Source composition may be a more important control on the Sr and Yb contents of syenites (Zhang et al., 2006). The Kuangdonggou diorites have higher Sr (1271–1339 ppm; average=1308 ppm) and Yb (1.61–2.20 ppm; average=1.83 ppm) contents than the syenites (Sr=665–766 ppm; average=704 ppm; Yb=3.44–3.63 ppm; average=3.52 ppm). This indicates that the addition of mantle-derived magma makes an important contribution to the Sr and Yb contents of the syenite, and that the crust-derived magma has a low Yb content. The post-tectonic I-type granitoids have low-Sr–low-Yb contents, reflecting a medium-pressure source. The S-type granitoids are low-Sr–high-Yb rocks, suggesting a low-pressure source. The Housongshugou pluton has high Sr/Yb ratios and plots in the field for adakitic rocks in a Y versus Sr/Y diagram, indicating that it was derived from thickened lower crust. Although the I-type granitoids were also derived from lower crust, they had a shallower source than the

Housongshugou pluton. The S-type granitoids were most likely derived by partial melting of meta-sedimentary rocks within the JLJB, and had the shallowest source. The post-tectonic granitoids have considerable variation in magma temperature with values of  $704$ – $726^\circ\text{C}$  for Housongshugou granodiorites,  $769$ – $791^\circ\text{C}$  for Nantaizi quartz monzonites,  $790$ – $908^\circ\text{C}$  for porphyritic monzogranite (except the Wolongquan pluton), and  $663$ – $801^\circ\text{C}$  for Wolongquan porphyritic monzogranite, respectively (Watson and Harrison, 1983).

## 5 Nature and Evolution of the Jiao–Liao–Ji Belt

### 5.1 Tectonic setting

In Y–Nb–Ce and Y–Nb–3Ga diagrams, almost all the pre-tectonic A-type granitoids plot in the  $A_2$  field (Fig. 11). The  $A_1$ -subtype is associated with mantle plumes and forms along rift zones, whereas the  $A_2$ -subtype occurs in extensional environments associated with post-orogenic and post-collisional settings (Eby, 1990, 1992). The  $A_2$ -subtype represents partial melting of crustal material in post-collisional or back-arc basin settings (Eby, 1992). The pre-tectonic adakitic rocks display depletion in Nb, Ta, and Ti, which is consistent with the Liaoji granitoids being related to a volcanic arc. The Liaoji granitoids comprise  $A_2$ -type granitoids and adakitic rocks. The assemblage of  $A_2$ -type granitoids and adakitic rocks, as well as contemporaneous calc-alkaline mafic rocks, indicates a back-arc basin or post-orogenic setting (Pearce et al., 1984; Deng et al., 2007; Dong et al., 2012; Meng et al., 2014; Yuan et al., 2015; Chen et al., 2016; Wang et al., 2016; Xu et al., 2018a–b). In combination with the evolutionary history of the JLJB inferred from detrital and magmatic zircons, a back-arc basin is the most plausible setting.

In Y–Nb–Ce and Y–Nb–3Ga diagrams, the post-tectonic A-type granitoids also plot in the  $A_2$  field (Fig. 11). I-type granitoids can form in various tectonic environments, whereas S-type granitoids are typically collisional granitoids (Chappell and White, 1992). Post-collisional alkalic rocks contain mafic minerals, and have high Ba and Sr contents, whereas anorogenic alkalic rocks have high Fe and low Ba and Sr contents (Sylvester, 1989; Bonin, 1990). The Kuangdonggou syenites contain biotite, amphibole, and pyroxene, and have high Sr (665–766 ppm) and Ba (1178–1980 ppm) contents, suggesting a post-collisional setting (Yang et al., 2007). The assemblage of  $A_2$ -, I-, and S-type, and adakitic rocks provides further evidence for a post-collisional setting. Based on the  $\sim 1.90$  Ga granulite-facies metamorphic rocks and clockwise metamorphic  $P$ – $T$ – $t$  paths of the meta-sedimentary rocks in the JLJB, the peak metamorphic age of the orogeny was between 1.95 and 1.90 Ga (Liu et al., 2013, 2015). Thus, the 1.90–1.80 Ga granitoids in the JLJB formed during the post-collisional stage.

### 5.2 Evolution of the Jiao–Liao–Ji Belt

Based on the widespread pre-tectonic A-type granitoids and bimodal volcanic rocks, an intra-continental rift model was proposed to describe the evolution of the JLJB (Zhang and Yang, 1988; Li and Zhao, 2007). However, the A-type

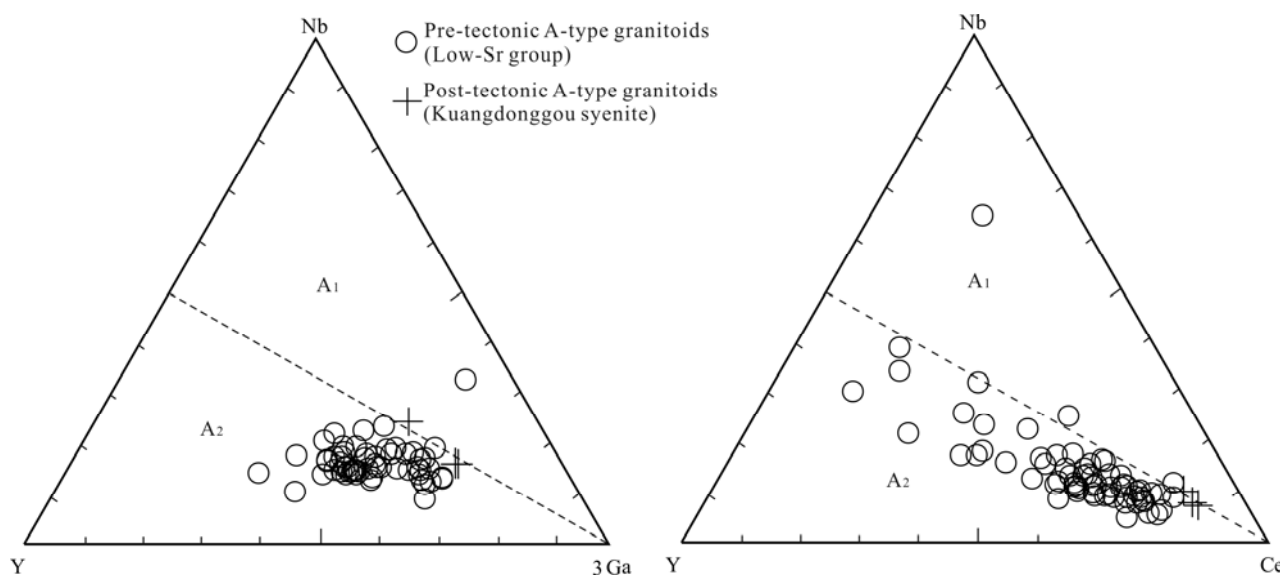


Fig. 11. Representative ternary diagrams for distinguishing between A<sub>1</sub> and A<sub>2</sub> granitoids (after Eby, 1992).

granitoids in the JLJB are the A<sub>2</sub>-subtype, which is considered to be associated with magmatism along a plate margin or island arc (Zhu et al., 2019). Based on newly discovered ~2.15 Ga meta-andesites, some studies have proposed that the bimodal volcanic rocks are actually a continuous magmatic sequence (Chen et al., 2016). Furthermore, all the igneous rocks in the JLJB are depleted in Nb, Ta, and Ti, reflecting a subduction affinity (Liu et al., 2013; Li and Chen, 2014; Chen et al., 2016; Meng et al., 2017a, c; Xu et al., 2019). As a result, an arc- or continent-continent collisional model has been proposed. This model considered the JLJB was a N-S-trending active continental margin that developed along the margin of the Longgang Block, and that the northern Longgang and southern Liaonan-Nangrim blocks were different Archean continental blocks separated by an ocean (Bai, 1993). However, this is inconsistent with zircon U-Pb ages and Hf isotopic data, which suggest that the Longgang and Liaonan-Nangrim blocks are similar Archean continental blocks (Luo et al., 2008; Zhao et al., 2012). The earlier models were refined to explain these new results. A rift-and-collision model was advocated by Zhao et al. (2012), which emphasized the tectonic transition from the early rifting event (2.2–1.9 Ga) to the subsequent arc-continent collision (1.9–1.8 Ga). The presence of 2.0 Ga adakitic rocks in the Huanghuadian area suggests that subduction had begun at 2.0 Ga (Wang P S et al., 2017; Liu J et al., 2018). This model can explain the similar Archean basement of the North and South Liaohe groups, the pre-tectonic A-type granitoids, and the ~1.90 Ga high-pressure metamorphic rocks. However, it is difficult to explain the presence of subduction-related mafic volcanic rocks. Thus, Wang et al. (2015) proposed that the JLJB was a back-arc basin between an eastern active continental arc (Rangnim Block) and a western Archean block (Longgang Block). The active continental arc separated from the Longgang Block, which formed the Rangnim Block. This model is supported by the

assemblage of pre-tectonic A<sub>2</sub>-type granitoids and adakitic rocks, as well as the different metamorphic *P-T-t* paths of the North and South Liaohe groups (Lu et al., 2006; Zhu et al., 2019). Thus, the initial tectonic setting of the JLJB was most likely a continental back-arc basin.

Based on paleomagnetism and large igneous provinces studies, the eastern (-northern) margin of the Sino-Korean Craton was considered to be of a close connection with the West Australian Craton (WAC) and/or North Australian Craton (NAC) during the Paleoproterozoic to Mesoproterozoic (1.78–1.40 Ga) (Zhang S H et al., 2012, 2017; Xu et al., 2014). Northwestward subduction of a Paleoproterozoic oceanic plate between the Eastern Block and West Australian Craton (WAC) and/or North Australian Craton (NAC) resulted in the extension of the back-arc basin (i.e., the JLJB) along the southeastern margin of the Eastern Block (2.20 to 2.10 Ga; Fig. 12a; Xu et al., 2019). In the later stages, the JLJB began to close at 2.10–2.00 Ga (Fig. 12b), which was followed by arc-continent collision at 2.00–1.90 Ga (Fig. 12c) and post-collisional extension from 1.90 to 1.80 Ga (Fig. 12d–e). The peak metamorphic age of metamorphism is ca. 1.95–1.90 Ga. A variety of granitoids formed in the post-collisional stage, including high- to low-pressure types. Crustal extension would have caused thinning of the crust and upwelling of mantle, resulting in an anomalously high heat flux. Partial melting of thickened crust is considered to be diagnostic of a transition in tectonic regime from compression to extension (Keay et al., 2001). Craven and Daczko (2018; pp. 1) advocated that “mantle-derived magmas are predicted to more readily migrate to shallower crustal levels as the crust thins and becomes hotter”. Therefore, the 2.20–2.15 Ga A<sub>2</sub>-type granitoids and adakitic rocks record the initial stage of back-arc extension, and represent the transition in tectonic regime from a passive to active continental margin setting (Zhu et al., 2019). The subsequent mafic intrusions (2.15–2.10 Ga) were intruded during peak back-arc extension (Xu et

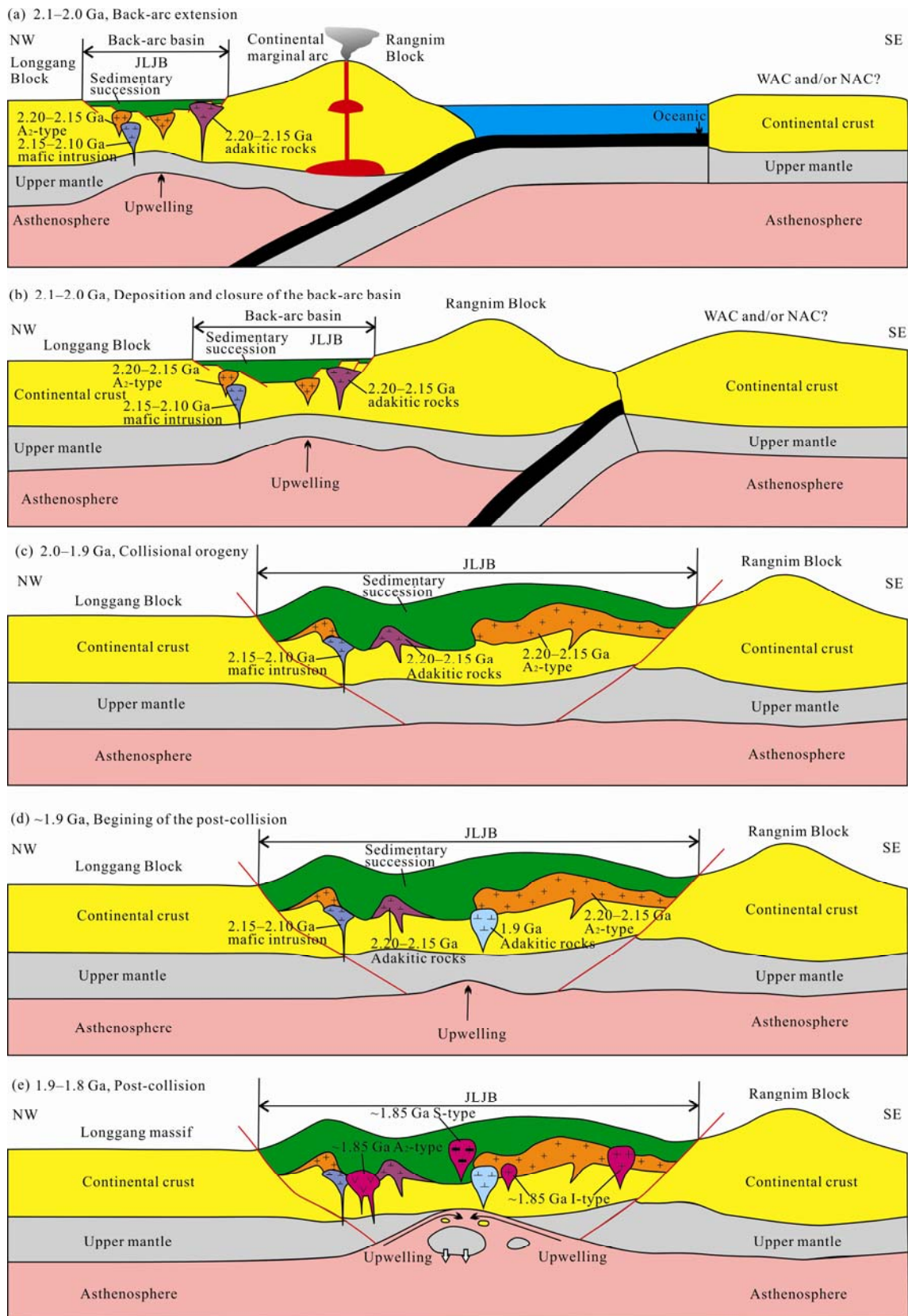


Fig. 12. Tectonic evolution of the JLJB (see text for details; after Zhu et al., 2019).

al., 2019). The ~1.90 Ga adakitic rocks (1892 Ma; high-Sr–low-Yb; high-pressure; 704–726°C) mark the beginning of the post-collisional stage, and were followed by the low-temperature S-type (1888.4 Ma; 663–801°C) and I-type (1850 Ma; 769–791°C) granitoids (low-Sr–low-Yb; medium-pressure). The presence of high-temperature granitoids (S-type; 1872–1859 Ma; low-Sr–high-Yb; low-pressure; 790–908°C) indicates the climax of post-collisional lithospheric delamination and asthenospheric upwelling. The crust-derived magma of the Kuangdonggou pluton (A<sub>2</sub>-type; 1879–1843 Ma) has low-Yb features, indicating it was coeval with the low-temperature group. Emplacement of the granitic pegmatites (1876–1740 Ma) was associated with the end of the orogeny.

## 6 Present Issues

### 6.1 Field contact relationships

Although numerous field geology, petrographic, geochronological, and geochemical studies of rocks in the JLJB have been undertaken, numerous issues remain controversial. One of the most controversial issues is the relationship between the Liaoji granitoids and meta-sedimentary rocks. Based on the ~2.15 Ga peak age of detrital zircons in the meta-sedimentary rocks, the Liaoji granitoids were considered to be basement and the provenance of the meta-sedimentary rocks (e.g., Lu, 2004; Luo et al., 2004, 2008; Lu et al., 2006; Liu et al., 2015). However, field investigations have indicated that most observed contact relationships were faulted rather than intrusive in nature. The lower Liaohe Group (Lieryu and Gaojiayu formations) is intruded by the Liaoji granitoids in the Sanjiazi area (Wang et al., 2015). A recent study indicated that the Na-rich granitoids are in fault contact with the Gaixian Formation (Zhu et al., 2019). As a result, some studies have proposed that the Liaoji granitoids intrude the Liaohe Group. In addition, some xenoliths of the Liaohe Group can be found in pre-tectonic plutons, demonstrating the Liaoji granitoids are younger than the Liaohe Group. These apparent intrusive contacts have been questioned by some studies, due to the strong overprinting by later thermal and tectonic events (Liu et al., 2015).

Uncertainties in locating the boundaries of different plutons are also problematic. Some samples having distinct mineralogical and geochemical compositions will be misidentified as coming from the same pluton due to the uncertainties in these boundaries (e.g., the two anomalous samples of the Wolongquan pluton, the sporadic adakitic samples in plutons that are composed mainly of A<sub>2</sub>-type granitoids, and the ~2.15 Ga monzogranitic gneiss and ~1.85 Ga porphyritic monzogranite in Jiguanshan pluton; Table 1) (Li and Zhao, 2007; Yang et al., 2015a; Song et al., 2016; Liu et al., 2017, 2018b).

### 6.2 Adakitic rocks

The formation age of the adakitic rocks is another outstanding issue. The Paleoproterozoic adakitic rocks can provide important constraints on the tectonic evolution of

the JLJB. Most of the Paleoproterozoic granitoids in the JLJB have single zircon age peaks, whereas some have complex zircon age distributions. The Paleoproterozoic granitoids with complex zircon age distributions include the Mafeng pluton (Li and Zhao, 2007), Fangjiaweizi and Dadingzi plutons (Song et al., 2016; Zhu et al., 2019), part of the Simenzi pluton (Song et al., 2016), and Housongshugou pluton (Ren et al., 2017). Most of these plutons are composed of adakitic granitoids, except for the Mafeng pluton. Zircons in these adakitic rocks can be divided into three groups: Archean, ~2.15 Ga, and ~1.85 Ga zircons (Li and Zhao, 2007; Song et al., 2016; Ren et al., 2017; Zhu et al., 2019). The Archean zircons are interpreted as being inherited, but the origin of the other two age groups is still controversial. Some studies consider that the ~2.15 and ~1.85 Ga zircons are of magmatic and metamorphic origin, respectively (Li and Zhao, 2007; Zhu et al., 2019). However, other studies consider that the ~2.15 Ga zircons are inherited, and that the ~1.85 Ga zircons are magmatic (Ren et al., 2017). For example, Song et al. (2016) suggested that the Dadingzi pluton formed at ~1.85 Ga, whereas Zhu et al. (2019) defined the age of this pluton as ~2.15 Ga (Table 1). Another possibility is that both ~2.15 and ~1.85 Ga adakitic rocks are present in the JLJB, such as the ~2.15 Ga Dadingzi and ~1.85 Ga Housongshugou plutons (Ren et al., 2017; Zhu et al., 2019). Although a large amount of age data has been obtained from the adakitic rocks, the primary contact relationships between the Liaohe Group and granodiorites has not been observed. Sporadic adakitic samples in some large pre-tectonic A<sub>2</sub>-type plutons suggest that the Paleoproterozoic adakitic rocks are more widespread than previously thought.

### 6.3 Origin of 2.10–1.95 Ga zircons

Some 2.10–1.95 Ga zircons are present in the granitoids that have complex zircon compositions, and also can be found in most meta-sedimentary and volcanic rocks (e.g., Lu et al., 2006; Li and Zhao, 2007; Xie et al., 2014; Liu et al., 2015; Meng et al., 2017a–c; Li et al., 2019). Based on the similar Hf isotopic compositions of the 2.10–1.95 and 2.2–2.1 Ga zircons in amphibolite and biotite–plagioclase gneiss (Ji'an Group), Meng et al. (2017a) proposed that these zircons have a similar origin. The 2.10–1.95 Ga zircons resulted from re-crystallization of 2.2–2.1 Ga magmatic zircons during metamorphic events, and the 1.9–1.8 Ga zircons were interpreted as new grains of metamorphic zircon due to their low Th/U ratios. Some studies have suggested that the 2.10–1.95 Ga detrital zircons were derived from igneous rocks (Luo et al., 2008; Meng et al., 2013). Although 2.10–1.95 Ga igneous rocks have been found in some areas, their scale is very small (Wang P S et al., 2017; Wang C C et al., 2017). Thus, it is difficult to explain the large number of 2.10–1.95 Ga detrital zircons in some of the meta-sedimentary rocks (Luo et al., 2006; Luo et al., 2008; Meng et al., 2013).

Detailed field investigations and zircon studies are the key to resolving these issues and, in particular, *in situ* zircon Hf and O isotopic studies. Although numerous age data have been reported, little Hf isotopic data is presently available. Most of the available Hf isotope data are from

magmatic zircons, and little data is available for metamorphic zircons. In addition, no O isotope studies have been undertaken on the Paleoproterozoic granodiorites of the JLJB. Sections that contain Paleoproterozoic granitoids and metamorphosed volcanic–sedimentary rocks should be identified and continuously sampled. Systematic U–Pb dating, geochemical, and isotopic studies should then be undertaken to resolve these outstanding issues.

## 7 Conclusions

A review of the field occurrence, petrography, geochronology, and geochemistry of Paleoproterozoic granitoids on Liaodong Peninsula, northeast China, allows us to reconstruct the tectonic evolution of the JLJB and reach the following conclusions.

(1) A variety of Paleoproterozoic granitoids occur in the Liaodong Peninsula, and can be divided into pre- and post-tectonic granitoids. The pre-tectonic granitoids comprise ~2.15 Ga monzogranite and granodiorite, and the post-tectonic granitoids comprise ~1.85 Ga monzogranite, granodiorite, porphyritic monzogranite, syenite, diorite, quartz monzonite, and granitic pegmatite.

(2) The pre-tectonic syenogranite and monzogranite are A<sub>2</sub>-type, and the pre-tectonic granodiorite has an adakitic affinity. The post-tectonic granitoids comprise adakitic (granodiorite), A<sub>2</sub>-type (syenite and diorite), I-type (quartz monzonite), and S-type (porphyritic monzogranite) rocks.

(3) The pre-tectonic adakitic and A<sub>2</sub>-type granitoids were derived from thickened and thinned lower crust, respectively. The post-tectonic adakitic and I-type granitoids were derived from lower crust, whereas the S-type granitoids were generated from upper crust. The post-tectonic A<sub>2</sub>-type granitoids resulted from mixing of crust- and mantle-derived magmas.

(4) The assemblage of pre-tectonic adakitic and A<sub>2</sub>-type granitoids indicate a continental back-arc basin setting, and the assemblage of post-tectonic adakitic and A<sub>2</sub>-, I-, and S-type granitoids indicate a post-collisional tectonic setting.

(5) The presence of pre-tectonic adakitic rocks (~2.17 Ga), in combination with A<sub>2</sub>-type granitoids, records a transition in tectonic regime from a passive to active continental margin setting.

(6) The presence of post-tectonic adakitic rocks (1892 Ma) signals the transition in tectonic regime from collision and compression to post-collisional extension, and was followed by emplacement of low-temperature S- and I-type granitoids. The high-temperature S-type granitoids were produced at the peak of post-collisional extension. Emplacement of the granitic pegmatites occurred at the end of the orogeny.

## Acknowledgements

The authors are grateful to editors and two anonymous reviewers for their extensive and insightful reviews and constructive comments that lead to significant improvement of the manuscript. This study was financially supported by the 3D Geological Mapping and

Deep Geological Survey of the China Geological Survey under a pilot project entitled Deep Geological Survey of the Benxi–Linjiang Area (Project No. 1212011220247).

Manuscript received May 15, 2019

accepted Aug. 14, 2019

associate EIC XIAO Wenjiao

edited by FEI Hongcai

## References

- Bai, J., 1993. The precambrian geology and Pb–Zn mineralization in the northern margin of North China Platform. Beijing: Geological Publishing House, 47–89 (in Chinese).
- Bi, J.H., Ge, W.C., Xing, D.H., Yang, H., Dong, Y., Tian, D.X., and Chen, H.J., 2018. Palaeoproterozoic meta-rhyolite and meta-dacite of the Liaohe Group, Jiao-Liao-Ji Belt, North China Craton: petrogenesis and implications for tectonic setting. *Precambrian Research*, 314: 306–324.
- Bonin, B., 1990. From orogenic to anorogenic settings: evolution of granitoid suites after a major orogenesis. *Geological Journal*, 25(3–4): 261–270.
- Boynnton, W.V., 1984. Geochemistry of the Rare Earth Elements: Meteorite Studies. In: Henderson, P. (ed.), *Rare Earth Elements Geochemistry*. Elsevier, Amsterdam, pp. 63–114.
- Chappell, B.W., and White, A.J.R., 1992. I- and S-type granites in the Lachlan Fold Belt. *Earth and Environmental Science Transactions of the Royal Society of Edinburgh*, 83(1–2): 1–26.
- Chappell, B.W., 1999. Aluminium saturation in I- and S-type granites and the characterization of fractionated haplogranites. *Lithos*, 46(3): 535–551.
- Chappell, B.W., and White, A.J.R., 2001. Two contrasting granite types: 25 years later. *Australian Journal of Earth Sciences*, 48(4): 489–499.
- Chen, B., Li, Z., Wang, J.L., and Yan, X.L., 2016. Liaodong Peninsula ~2.2 Ga magmatic event and its geological significance. *Journal of Jilin University (Earth Science Edition)*, 46(2): 303–320 (in Chinese with English abstract).
- Craven, S.J., and Daczko, N.R., 2018. High-temperature–low-pressure metamorphism and the production of S-type granites of the Hillgrove Supersuite, southern New England Orogen, NSW, Australia. *Australian Journal of Earth Sciences*, 65(5): 1–17.
- Defant, M.J., and Drummond, M.S., 1990. Derivation of some modern arc magmas by melting of young subducted lithosphere. *Nature*, 347(6294): 662–665.
- Deng, J.F., Xiao, Q.H., Su, S.G., Liu, C., Zhao, G.C., Wu, Z.X., and Liu, Y., 2007. Igneous petro-tectonic assemblages and tectonic settings: A discussion. *Geological Journal of China Universities*, 13(3): 392–402 (in Chinese with English abstract).
- Dong, C.Y., Ma, M.Z., Liu, S.J., Xie, H.Q., Liu, D.Y., Li, X.M., and Wan, Y.S., 2012. Middle Paleoproterozoic crustal extensional regime in the North China Craton: new evidence from SHRIMP zircon U–Pb dating and whole-rock geochemistry of meta-gabbro in the Anshan-Gongchangling area. *Acta Petrologica Sinica*, 28(9): 2785–2792 (in Chinese with English abstract).
- Eby, G.N., 1990. The A-type granitoids: A review of their occurrence and chemical characteristics and speculations on their petrogenesis. *Lithos*, 26(1): 115–134.
- Eby G.N., 1992. Chemical subdivision of the A-type granitoids: Petrogenetic and tectonic implications. *Geology*, 20(7): 641–644.
- Faure, M., Lin, W., Monie, P., and Bruguier, O., 2004. Paleoproterozoic arc magmatism and collision in Liaodong Peninsula (north–east China). *Terra Nova*, 16(2): 75–80.
- Feng, X.Z., Xiao, Y., and Liu, C.X., 2008. Geology and geochemistry of the Gaotaigou boron deposit in southern Jilin. *China Geology of Chemical Minerals*, 3(4): 207–216 (in Chinese with English abstract).
- Ge, W.C., Lin, Q., Fang, Z.R., 1991. A rapakivi by assimilation

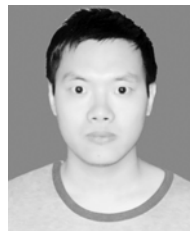
- and contamination in Kuandian, Liaoning Province, China. *Journal of Changchun University of Earth Science*, 21(2): 135–141 (in Chinese with English abstract).
- Ge, X.Y., Li, X.H., Chen, Z.G., Li, W.P., 2002. Geochemistry and petrogenesis of Jurassic high Sr/low Y granitoids in eastern China: Constrains on crustal thickness. *Chinese Science Bulletin*, 47(6): 474–480 (in Chinese).
- GSILP (Geological Survey Institute of Liaoning Province), 2019. 1:50000 scale geological maps of Shangmatun, Tianshui, Caohekou, Sanjiazi, Qingchengzi and Tongyuanpu, and the related notes (in Chinese).
- Hao, D.F., Li, S.Z., Zhao, G.C., Sun, M., Han, Z.Z., and Zhao, G.T., 2004. Origin and its constraint to tectonic evolution of Paleoproterozoic granitoids in the eastern Liaoning and Jilin province, North China. *Acta Petrologica Sinica*, 20(6): 1409–1416 (in Chinese with English abstract).
- He, G.P., and Ye, H.W., 1998. Two types of early Proterozoic metamorphism in the Eastern Liaoning and Southern Jilin provinces and their tectonic implications. *Acta Petrologica Sinica*, 14(2): 152–162 (in Chinese with English abstract).
- Keay, S., Lister, G., and Buick, I., 2001. The timing of partial melting, Barrovian metamorphism and granite intrusion in the Naxos metamorphic core complex, Cyclades, Aegean Sea, Greece. *Tectonophysics*, 342(3): 275–312.
- King, P.L., White, A.J.R., Chappell, B.W., and Allen, C.W., 1997. Characterization and origin of aluminous A-type granites from the Lachlan Fold Belt, Southeastern Australia. *Journal of Petrology*, 38(3): 371–391.
- Li, C., Li, Z., Yang, C., 2017a. Palaeoproterozoic granitic magmatism in the northern segment of the Jiao-Liao-Ji Belt: implications for orogenesis along the Eastern Block of the North China Craton. *International Geology Review*, 60: 217–241.
- Li, C., Chen, B., Li, Z., and Yang, C., 2017b. Petrologic and geochemical characteristics of Paleoproterozoic monzogranitic gneisses from Xiuyan-Kuandian area in Liaodong Peninsula and their tectonic implications. *Acta Petrologica Sinica*, 33(3): 963–977 (in Chinese with English abstract).
- Li, S.Z., Yang, Z.S., and Liu, Y.J., 1996. Preliminary analysis on uplift bedding delamination structure of the Palaeoproterozoic orogenic belt in Liaodong peninsula. *Journal of Changchun University of Earth Science*, 26(3): 305–309 (in Chinese with English abstract).
- Li, S.Z., Yang, Z.S., Liu, Y.J., and Liu, J.L., 1997. Emplacement model of Paleoproterozoic early granite in Jiao-Liao-Ji area and its relation to the uplift bedding delamination structural series. *Acta Petrologica Sinica*, 13(2): 189–202 (in Chinese with English abstract).
- Li, S.Z., Zhao, G.C., Sun, M., Han, Z.Z., Hao, D.F., Luo, Y., and Xia, X.P., 2005. Deformation history of the Paleoproterozoic Liaohe Group in the Eastern Block of the North China Craton. *Journal of Asian Earth Sciences*, 24(5): 659–674.
- Li, S.Z., Zhao, G.C., Sun, M., Han, Z.Z., Zhao, G.T., and Hao, D.F., 2006. Are the South and North Liaohe Groups different exotic terranes? –Nd isotope constraints on the Jiao-Liao-Ji orogen. *Gondwana Research*, 9(1–2): 198–208.
- Li, S.Z., and Zhao, G.C., 2007. SHRIMP U–Pb zircon geochronology of the Liaoji granitoids: Constraints on the evolution of the Paleoproterozoic Jiao-Liao-Ji belt in the Eastern Block of the North China Craton. *Precambrian Research*, 158(1–2): 1–16.
- Li, S.Z., Zhao, G.C., Santosh, M., Liu, X., Dai, L., Suo, Y.H., Tam, P.K., Song, M., and Wang, P.C., 2012. Paleoproterozoic structural evolution of the southern segment of the Jiao-Liao-Ji belt, North China Craton. *Precambrian Research*, 200–203 (4): 59–73.
- Li, X.H., Li, W.X., and Li, Z.X., 2007. Revisiting the genetic type and implication for tectonics of the early Yanshanian granites in Nanling area. *Chinese Science Bulletin*, 52(9): 981–991 (in Chinese).
- Li, W.X., and Li, X.H., 2003. Rock types and tectonic significance of the granitoids rocks within ophiolites. *Advance in Earth Sciences*, 18(3): 392–397 (in Chinese with English abstract).
- Li, Z., and Chen, B., 2014. Geochronology and geochemistry of the Paleoproterozoic meta-basalts from the Jiao-Liao-Ji Belt, North China Craton: Implications for petrogenesis and tectonic setting. *Precambrian Research*, 255: 653–667.
- Li, Z., Chen, B., Liu, J.W., Zhang, L., and Yang, C., 2015a. Zircon U–Pb ages and their implications for the South Liaohe Group in the Liaodong Peninsula, Northeast China. *Acta Petrologica Sinica*, 31(6): 1589–1605 (in Chinese with English abstract).
- Li, Z., Chen, B., Wei, C.J., Wang, C.X., and Han, W., 2015b. Provenance and tectonic setting of the Paleoproterozoic metasedimentary rocks from the Liaohe Group, Jiao-Liao-Ji Belt, North China Craton: Insights from detrital zircon U–Pb geochronology, whole-rock Sm–Nd isotopes, and geochemistry. *Journal of Asian Earth Sciences*, 111: 711–732.
- Li, Z., and Chen, B., 2016. Geochronological framework and geodynamic implications of mafic dykes in the Liaodong Peninsula, North China Craton. *Acta Geologica Sinica (English Edition)*, 90(S1): 76–77.
- Li, Z., Chen, B., and Wang, J.L., 2016. Geochronological framework and geodynamic implications of mafic magmatism in the Liaodong Peninsula and adjacent regions, North China Craton. *Acta Geologica Sinica (English Edition)*, 90(1): 138–153.
- Li, Z., Chen, B., and Wei, C.J., 2017. Is the Paleoproterozoic Jiao-Liao-Ji Belt (North China Craton) a rift? *International Journal of Earth Sciences*, 106(1): 355–375.
- Li, Z., Chen, B., and Yan X.L., 2019. The Liaohe Group: An insight into the Paleoproterozoic tectonic evolution of the Jiao-Liao-Ji Belt, North China Craton. *Precambrian Research*, 326: 174–195.
- Liu, D.Y., Nutman, A.P., Compston, W., Wu, J.S., and Shen, Q.H., 1992. Remnants of > 3800 Ma crust in the Chinese part of the Sino-Korean Craton. *Geology*, 20(4): 339–342.
- Liu, J.D., Xiao, R.G., Wang, W.W., and Wang, C.Z., 2007. Regional Metallogenesis of Borate Deposit in Eastern Liaoning. Beijing: Geological Publishing House (in Chinese with English abstract).
- Liu, P.H., Liu, F.L., Wang, F., and Liu, J.H., 2010. Genetic mineralogy and metamorphic evolution of mafic high-pressure (HP) granulites from the Shandong Peninsula, China. *Acta Petrologica Sinica*, 26(7): 2039–2056 (in Chinese with English abstract).
- Liu, P.H., Liu, F.L., Wang, F., and Liu, J.H., 2011a. U–Pb dating of zircons from Al-rich paragneisses of Jingshan Group in Shandong peninsula and its geological significance. *Acta Petrologica Et Mineralogica*, 30(5): 829–843 (in Chinese with English abstract).
- Liu, P.H., Liu, F.L., Wang, F., and Liu, J.H., 2011b. In-situ U–Pb dating of zircons from high-pressure granulites in Shandong Peninsula, Eastern China and its geological significance. *Earth Science Frontiers*, 18(2): 33–54 (in Chinese with English abstract).
- Liu, P.H., Liu, F.L., Wang, F., Liu, J.H., Yang, H., and Shi, J.R., 2012. Geochemical characteristics and genesis of the high-pressure mafic granulite in the Jiaobei high-grade metamorphic basement, eastern Shandong, China. *Acta Petrologica Sinica*, 28(9): 2705–2720 (in Chinese with English abstract).
- Liu, P.H., Liu, F.L., Wang, F., Liu, J.H., and Cai, J., 2013. Petrological and geochronological preliminary study of the Xiliu ~2.1Ga meta-gabbro from the Jiaobei terrane, the southern segment of the Jiao-Liao-Ji Belt in the North China Craton. *Acta Petrologica Sinica*, 29(7): 2371–2390 (in Chinese with English abstract).
- Liu, F.L., Liu, P.H., Wang, F., Liu, C.H., and Cai, J., 2015. Progresses and overviews of voluminous meta-sedimentary series within the Paleoproterozoic Jiao-Liao-Ji orogenic/mobile belt, North China Craton. *Acta Petrologica Sinica*, 31(10): 2816–2846 (in Chinese with English abstract).
- Liu, F.L., Liu, C.H., Itano, K., Iizuka, T., Cai, J., and Wang, F., 2017. Geochemistry, U–Pb dating, and Lu–Hf isotopes of zircon and monazite of porphyritic granites within the Jiao-Liao-Ji orogenic belt: implications for petrogenesis and tectonic setting. *Precambrian Research*, 300: 78–106.

- Liu, J., Zhang, J., Liu, Z., Yin, C., Zhao, C., Li, Z., Yang, Z.J., and Dou, S.Y., 2018. Geochemical and geochronological study on the Paleoproterozoic rock assemblage of the Xiuyan region: New constraints on an integrated rift-and-collision tectonic process involving the evolution of the Jiao-Liao-Ji belt, North China Craton. *Precambrian Research*, 310: 179–197.
- Liu, W.B., Peng, Y.B., Zhao, C., Cui, Y.S., Yang, C.H., and Wen, C., 2018. LA-ICP-MS zircon U-Pb dating and geochemistry of Wolongquan intrusion in gaizhou, southern Liaoning Province. *Geology and Resources*, 27(6): 531–539 (In Chinese with English abstract).
- Lu, X.P., 2004. Paleoproterozoic tectonic magmatic event in Tonghua area. Ph. D. Dissertation. Changchun: Jilin University, 1–152 (in Chinese with English abstract).
- Lu, X.P., Wu, F.Y., Lin, J.Q., Sun, D.Y., Zhang, Y.B., and Guo, C.L., 2004a. Geochronological successions of the early Precambrian granitic magmatism in southern Liaodong peninsula and its constraints on tectonic evolution of the North China Craton. *Chinese Journal of Geology*, 39(1): 123–138 (in Chinese with English abstract).
- Lu, X.P., Wu, F.Y., Zhang Y.B., Zhao C.B., and Guo C.L., 2004b. Emplacement age and tectonic setting of the Paleoproterozoic Liaoji granites in tonghua area, southern Jilin Province. *Acta Petrologica Sinica*, 20(3): 381–392 (in Chinese with English abstract).
- Lu, X.P., Wu, F.Y., Guo, J.H., and Yin, C.J., 2005. Late Paleoproterozoic granitic magmatism and crustal evolution in the Tonghua region, northeast China. *Acta Petrologica Sinica*, 21(3): 721–736 (in Chinese with English abstract).
- Lu, X.P., Wu, F.Y., Guo, J.H., Wilde, S.A., Yang, J.H., Liu, X.M., and Zhang, X.O., 2006. Zircon U–Pb geochronological constraints on the Paleoproterozoic crustal evolution of the Eastern Block in the North China Craton. *Precambrian Research*, 146(3–4): 138–164.
- Luo, Y., Sun, M., Zhao, G.C., Li, S.Z., Xu, P., Ye, K., and Xia, X.P., 2004. LA-ICP-MS U–Pb zircon ages of the Liaohe Group in the Eastern Block of the North China Craton: Constraints on the evolution of the Jiao-Liao-Ji Belt. *Precambrian Research*, 134: 349–371.
- Luo, Y., Sun, M., Zhao, G.C., Li, S.Z., Ayers, J.C., Xia, X.P., and Zhang, J.H., 2008. A comparison of U–Pb and Hf isotopic compositions of detrital zircons from the North and South Liaohe Groups: constraints on the evolution of the Jiao-Liao-Ji Belt, North China Craton. *Precambrian Research*, 163: 279–306.
- Meng, E., Liu, F.L., Liu, J.H., Liu, P.H., Cui, Y., Liu, C.H., Yang, H., Wang, F., Shi, J.R., Kong, Q.B., and Lian, T.H., 2013. Zircon U–Pb and Lu–Hf isotopic constraints on Archean crustal evolution in the Liaonan Complex of northeast China. *Lithos*, 177(4): 164–183.
- Meng, E., Liu, F.L., Liu, P.H., Liu, C.H., Yang, H., Wang, F., Shi, J.R., and Cai, J., 2014. Petrogenesis and tectonic significance of Paleoproterozoic meta-mafic rocks from central Liaodong Peninsula, northeast China: Evidence from zircon U–Pb dating and in situ Lu–Hf isotopes, and whole-rock geochemistry. *Precambrian Research*, 247: 92–109.
- Meng, E., Wang, C.Y., Yang, H., Cai, J., Ji, L., and Li, Y.G., 2017a. Paleoproterozoic meta-volcanic rocks in the Ji'an Group and constraints on the formation and evolution of the northern segment of the Jiao-Liao-Ji Belt, China. *Precambrian Research*, 294: 133–150.
- Meng, E., Wang, C.Y., Li, Y.G., Li, Z., Yang, H., Cai, J., Ji, L., and Ji, M.Q., 2017b. Zircon U–Pb–Hf isotopic and whole-rock geochemical studies of Paleoproterozoic metasedimentary rocks in the northern segment of the Jiao-Liao-Ji Belt, China: Implications for provenance and regional tectonic evolution. *Precambrian Research*, 298: 472–489.
- Meng, E., Wang, C.Y., Liu, C.H., Shi, J.R., and Li, Y.G., 2017c. Geochronology, petrogenesis and constraints on regional tectonic evolution of the meta-volcanic rocks in southeastern Liaodong Peninsula. *Journal of Jilin University (Earth Science Edition)*, 47(6): 1589–1619 (in Chinese with English abstract).
- Patino, Douce, A.E., 1997. Generation of metaluminous A-type granites by low-pressure melting of calc-alkaline granitoids. *Geology*, 25: 743–746.
- Pearce, J.A., Harris, N.B.W., and Tindle, A.G., 1984. Trace element discrimination diagrams for the tectonic interpretation of granitic rocks. *Journal of Petrology*, 25(4): 956–983.
- Qin, Y., 2013. Geochronological Constraints in the Tectonic Evolution of the Liao-ji Paleoproterozoic rift zone. Ph. D. Dissertation. Changchun: Jilin University, 1–156 (in Chinese with English abstract).
- Ren, Y.W., Wang, H.C., Kang, J.L., Chu, H., and Tian, H., 2017. Paleoproterozoic magmatic events in the Hupiyu area in Yingkou, Liaoning province and their geological significance. *Acta Geologica Sinica*, 91(11): 2456–2472 (in Chinese with English abstract).
- Song, B., Nutman, A.P., Liu, D.Y., and Wu, J.S., 1996. 3800 to 2500 Ma crustal evolution in the Anshan area of Liaoning Province, northeastern China. *Precambrian Research*, 78: 79–94.
- Song, Y.H., Yang, F.C., Yan, G.L., Wei, M.H., and Shi, S.S., 2016. SHRIMP U–Pb ages and Hf Isotopic compositions of Paleoproterozoic granites from the eastern part of Liaoning province and their tectonic significance. *Acta Geologica Sinica*, 90(10): 2620–2636 (in Chinese with English abstract).
- Sun, S.S., and McDonough, W.F., 1989. Chemical and isotopic systematics of oceanic basalts: Implications for mantle composition and processes. *Geological Society Special Publication*, London, pp. 313–345.
- Sylvester, P.J., 1989. Post-collisional alkaline granites. *Journal of Geology*, 97(3): 261–280.
- Sylvester, P.J., 1998. Post-collisional strongly peraluminous granites. *Lithos*, 45(1): 29–44.
- Teng, D.W., Wang, Y.K., Hao, X.J., Liu, Z.H., and Zhu, K., 2017. Petrogenesis of Liaoji granites in Yongdian area of Liaoning and their constraints on tectonic evolution of Liao–Ji mobile belt. *Global Geology*, 36(4): 1100–1115 (in Chinese with English abstract).
- Wan, Y.S., Liu, D.Y., Wu, J.S., Zhang, Z.Q., and Song, B., 1998. The origin of Mesoarchean granitic rocks from Anshan-Benxi area: constraints of geochemistry and Nd isotope. *Acta Petrologica Sinica*, 14(3): 278–288 (in Chinese with English abstract).
- Wan, Y.S., Geng, Y.S., Shen, Q. H., Liu, D.Y., Tang, S.H., and Wang, J.H., 2002. Geochemical characteristics of supracrustal enclaves in Mesoarchean Tiejiaoshan granite of the Anshan area and its geological significance. *Scientia Geologica Sinica*, 37(2): 143–151 (in Chinese with English abstract).
- Wan, Y.S., Liu, D.Y., Song, B., Wu, J.S., Yang, C.H., Zhang, Z.Q., and Geng, Y.S., 2005. Geochemical and Nd isotopic compositions of 3.8 Ga meta-quartz dioritic and trondhjemitic rocks from the Anshan area and their geological significance. *Journal of Asian Earth Sciences*, 24(5): 563–575.
- Wan, Y.S., Song, B., Liu, D.Y., Wilde, S.A., Wu, J.S., Shi, Y.R., Yin, X.Y., and Zhou, H.Y., 2006. SHRIMP U–Pb zircon geochronology of Paleoproterozoic metasedimentary rocks in the North China Craton: evidence for a major Late Paleoproterozoic tectonothermal event. *Precambrian Research*, 149: 249–271.
- Wan, Y.S., Liu, D.Y., Yin, X.Y., Wilde, S.A., Xie, L.W., Yang, Y.H., Zhou, H.Y., and Wu, J.S., 2007. SHRIMP geochronology and Hf isotope composition of zircons from the Tiejiaoshan granites and supracrustal rocks in the Anshan area, Liaoning Province. *Acta Petrologica Sinica*, 23(2): 241–252 (in Chinese with English abstract).
- Wan, Y.S., Dong, C.Y., Liu, Y.D., Kröner, A., Yang, C.H., Wang, W., Du, L.L., Xie, H.Q., and Ma, M.Z., 2012a. Zircon ages and geochemistry of late Neoproterozoic syenogranites in the North China Craton: A review. *Precambrian Research*, 222–223: 265–289.
- Wan, Y.S., Liu, D.Y., Nutman, A., Zhou, H.Y., Dong, C.Y., Yin, X.Y., and Ma, M.Z., 2012b. Multiple 3.8–3.1 Ga tectono-magmatic events in a newly discovered area of ancient rocks (the Shengousi Complex), Anshan, North China Craton. *Journal of Asian Earth Sciences*, 54–55: 18–30.
- Wan, Y.S., Zhang, Y.H., Williams, I.S., Liu, D.Y., Dong, C.Y., Fan, R.L., Shi, Y.R., and Ma, M.Z., 2013. Extreme zircon O

- isotopic compositions from 3.8 to 2.5 Ga magmatic rocks from the Anshan area, North China Craton. *Chemical Geology*, 352: 108–124.
- Wan, Y.S., Ma, M.Z., Dong, C.Y., Xie, H.Q., Xie, S.W., Ren, P., and Liu, D.Y., 2015. Widespread late Neoproterozoic reworking of Meso- to Paleoproterozoic continental crust in the Anshan-Benxi area, North China Craton, as documented by U–Pb–Nd–Hf–O isotopes. *American Journal of Science*, 315(7): 620–670.
- Wang, C.C., Liu, Y.C., Zhang, P.G., Zhao, G.C., Wang, A.D., and Song, B., 2017. Zircon U–Pb geochronology and geochemistry of two types of Paleoproterozoic granitoids from the southeastern margin of the North China Craton: constraints on petrogenesis and tectonic significance. *Precambrian Research*, 303: 268–290.
- Wang, F., Liu, F.L., Liu, P.H., Cai, J., Schertl, H.P., Ji, L., Liu, L.S., and Tian, Z.H., 2017. In situ zircon U–Pb dating and whole-rock geochemistry of metasedimentary rocks from South Liaohe Group, Jiao-Liao-Ji orogenic belt: Constraints on the depositional and metamorphic ages, and implications for tectonic setting. *Precambrian Research*, 303: 764–780.
- Wang, H.C., Lu, S.N., Chu, H., Xiang, Z.Q., Zhang, C.J., and Liu, H., 2011. Zircon U–Pb age and tectonic setting of metabasalts of Liaohe Group in Helan area, Liaoyang, Liaoning Province. *Journal of Jilin University (Earth Science Edition)*, 41(5): 1322–1334 (in Chinese with English abstract).
- Wang, H.C., Ren, Y.W., Lu, S.N., Kang, J.L., Chu, H., Yu, H.B., and Zhang, C.J., 2015. Stratigraphic units and tectonic setting of the Paleoproterozoic Liao-Ji orogen. *Acta Geoscientia Sinica*, 36(5): 583–598 (in Chinese with English abstract).
- Wang, M.J., Liu, S.W., Fu, J.H., Wang, K., Guo, R.R., and Guo, B.R., 2017. Neoproterozoic DTG gneisses in southern Liaoning Province and their constraints on crustal growth and the nature of the Liao-Ji Belt in the Eastern Block. *Precambrian Research*, 303: 183–207.
- Wang, P.S., Dong, Y.S., Li, F.Q., Gao, B.S., Gan, Y.C., Chen, M.S., and Xu, W., 2017. Paleoproterozoic granitic magmatism and geological significance in Huanghuadian area, eastern Liaoning Province. *Acta Petrologica Sinica*, 33(9): 2708–2724 (in Chinese with English abstract).
- Wang, W., Yang, H., and Ji, L., 2017. The identification of the Neoproterozoic 2.52–2.46 Ga tectono-thermal events from the Liaonan terrain and its geological significance. *Acta Petrologica Sinica*, 33(9): 2775–2784 (in Chinese with English abstract).
- Wang, X.J., Liu, J.H., and Ji, L., 2017. Zircon U–Pb chronology, geochemistry and their petrogenesis of Paleoproterozoic monzogranitic gneisses in Kuandian area, eastern Liaoning Province, Jiao-Liao-Ji Belt, North China Craton. *Acta Petrologica Sinica*, 33(9): 2689–2707 (in Chinese with English abstract).
- Wang, X.P., Peng, P., Wang, C., and Yang, S.Y., 2016. Petrogenesis of the 2115 Ma Haicheng mafic sills from the Eastern North China Craton: implications for an intra-continental rifting. *Gondwana Research*, 39: 347–364.
- Wang, X.P., Peng, P., Wang, C., and Yang, S.Y., 2017. Nature of three episodes of Paleoproterozoic magmatism (2180 Ma, 2115 Ma and 1890 Ma) in the Liaoji belt, North China with implications for tectonic evolution. *Precambrian Research*, 298: 252–267.
- Whalen, J.B., Currie, K.L., and Chappell, B.W., 1987. A-type granites: Geochemical characteristics, discrimination and petrogenesis. *Contributions to Mineralogy and Petrology*, 95(4): 407–419.
- Wu, J. S., Geng, Y. S., Shen, Q. H., Wan, Y. S., Liu, D. Y., and Song, B., 1998. Archean geology characteristics and tectonic evolution of China-Korea Paleo-continent. Beijing: Geological Publishing House (in Chinese).
- Wu, F.Y., Li, X.H., Yang, J.H., and Zheng, Y.F., 2007. Discussion on the petrogenesis of granites. *Acta Petrologica Sinica*, 23(6): 1217–1238.
- Wu, F.Y., Zhang, Y.B., Yang, J.H., Xie, L.W., and Yang, Y.H., 2008. Zircon U–Pb and Hf isotopic constraints on the Early Archean crustal evolution in Anshan of the North China Craton. *Precambrian Research*, 167: 339–362.
- Wu, F.Y., Li, Q.L., Yang, J.H., Kim, J.N., and Han, R.H., 2016. Crustal growth and evolution of the Rangnim Massif, northern Korean Peninsula. *Acta Petrologica Sinica*, 32(10): 2933–2947 (in Chinese with English abstract).
- Xia, X.P., Sun, M., Zhao, G.C., and Luo, Y., 2006a. LA-ICP-MS U–Pb geochronology of detrital zircons from the Jining Complex, North China Craton and its tectonic significance. *Precambrian Research*, 144: 199–212.
- Xia, X.P., Sun, M., Zhao, G.C., Wu, F.Y., Xu, P., Zhang, J.H., and Luo, Y., 2006b. U–Pb and Hf isotopic study of detrital zircons from the Wulashan khondalites: Constraints on the evolution of the Ordos Terrane, western block of the North China Craton. *Earth & Planetary Science Letters*, 241(3): 581–593.
- Xie, S.W., Wang, S.J., Xie, H.Q., Liu, S.J., Dong, C.Y., Ma, M.Z., Liu, D.Y., and Wan, Y.S., 2014. SHRIMP U–Pb dating of detrital zircons from the Fenzishan Group in eastern Shandong, North China craton. *Acta Petrologica Sinica*, 30(10): 2989–2998 (In Chinese with English abstract).
- Xu, H.R., Yang, Z.Y., Peng, P., Meert, J.G., and Zhu, R.X., 2014. Paleo-position of the North China craton within the supercontinent Columbia: constraints from new paleomagnetic results. *Precambrian Research*, 255: 276–293.
- Xu, W., Liu, F.L., Tian, Z.H., Liu, L.S., Ji, L., and Dong, Y.S., 2018a. Source and petrogenesis of Paleoproterozoic meta-mafic rocks intruding into the North Liaohe Group: implications for back-arc extension prior to the formation of the Jiao-Liao-Ji Belt, North China Craton. *Precambrian Research*, 307: 66–81.
- Xu, W., Liu, F.L., Santosh, M., Liu, P.H., Tian, Z.H., and Dong, Y.S., 2018b. Constraints of mafic rocks on a Paleoproterozoic back-arc in the Jiao-Liao-Ji Belt, North China Craton. *Journal of Asian Earth Sciences*, 166: 195–209.
- Xu, W., and Liu, F.L., 2019. Geochronological and geochemical insights into the tectonic evolution of the Paleoproterozoic Jiao-Liao-Ji Belt, Sino-Korean Craton. *Earth-Science Reviews*, 193: 162–198.
- Yang, J.H., Chung, S.L., Wilde, S.A., Wu, F.Y., Chu, M.F., Lo, C.H., and Fan, H.R., 2005. Petrogenesis of post-orogenic syenites in the Sulu Orogenic Belt, East China: geochronological, geochemical and Nd–Sr isotopic evidence. *Chemical Geology*, 214: 99–125.
- Yang, J.H., Wu, F.Y., Xie, L.W., and Liu, X.M., 2007. Petrogenesis and tectonic implications of Kuangdonggou syenites in the Liaodong Peninsula, east North China Craton: constraints from in-situ zircon U–Pb ages and Hf isotopes. *Acta Petrologica Sinica*, 23(2): 263–276 (in Chinese with English abstract).
- Yang, M.C., Chen, B., and Yan, C., 2015a. Petrogenesis of Paleoproterozoic gneissic granites from Jiao-Liao-Ji Belt of North China Craton and their tectonic implications. *Journal of Earth Sciences and Environment*, 37(5): 31–51 (in Chinese with English abstract).
- Yang, M.C., Chen, B., and Yan, C., 2015b. Petrological, geochronological, geochemical and Sr–Nd–Hf isotopic constraints on the petrogenesis of the Shuangcha Paleoproterozoic megaporphyritic granite in the southern Jilin Province: tectonic implications. *Acta Petrologica Sinica*, 31(6): 1573–1588 (in Chinese with English abstract).
- Yang, M.C., Chen, B., Yan, C., 2016. Paleoproterozoic gneissic granites in the Liaoji Mobile belt, North China Craton: implications for tectonic setting. In: Zhai, M.G., Zhao, Y., and Zhao, T.P. (eds.), *Main Tectonic Events and Metallogeny of the North China Craton*. Springer, pp. 155–180.
- Yang H., Wang, W., and Liu, J.H., 2017. Zircon U–Pb dating and its geological significance of granitic pegmatites from the Kuandian and Sanjiazi area in eastern Liaoning Province. *Acta Petrologica Sinica*, 33(9): 2675–2688 (in Chinese with English abstract).
- Yuan, L.L., Zhang, X.H., and Zhai, M.G., 2015. Two episodes of Paleoproterozoic mafic intrusions from Liaoning province, North China Craton: petrogenesis and tectonic implications. *Precambrian Research*, 264, 119–139.
- Zhang, Q.S., and Yang, Z.S., 1988. Early crust and mineral deposits of Liaodong Peninsula. Beijing: Geological

- Publishing House, pp. 218–450 (in Chinese with English abstract).
- Zhang, Q., Wang, Y., Li, C.D., Wang, Y.L., Jin, W.J., and Jia, X.Q., 2006. Granite classification on the basis of Sr and Yb contents and its implications. *Acta Petrologica Sinica*, 22(9): 2249–2269 (in Chinese with English abstract).
- Zhang, Q., Ran, H., and Li, C.D., 2012. A-type granite: What is the essence? *Acta Petrologica Et Mineralogica*, 31(4): 621–626 (in Chinese with English abstract).
- Zhang, S.H., Li, Z.X., Evans, D.A.D., Wu, H.C., Li, H.Y., and Dong, J., 2012. Pre-Rodinia supercontinent Nuna shaping up: a global synthesis with new paleomagnetic results from North China. *Earth and Planetary Science Letters*, 353–354: 145–155.
- Zhang, S.H., Zhao, Y., Li, X.H., Ernst, R.E., and Yang, Z.Y., 2017. The 1.33–1.30 Ga Yanliao large igneous province in the North China Craton: Implications for reconstruction of the Nuna (Columbia) supercontinent, and specifically with the North Australian Craton. *Earth and Planetary Science Letters*, 465: 112–125.
- Zhao, G.C., Simon, A.W., and Cawood, P.A., 1998. Thermal evolution of Archean basement rocks from the eastern part of the North China Craton and its bearing on tectonic setting. *International Geology Review*, 40(8): 706–721.
- Zhao, G.C., Wilde, S.A., Cawood, P.A., and Sun, M., 2001. Archean blocks and their boundaries in the North China Craton: lithological, geochemical, structural and P-T path constraints and tectonic evolution. *Precambrian Research*, 107: 45–73.
- Zhao, G.C., Wilde, S.A., Cawood, P.A., and Sun, M., 2002. SHRIMP U–Pb zircon ages of the Fuping Complex: implications for accretion and assembly of the North China Craton. *American Journal of Science*, 302: 191–226.
- Zhao, G.C., Sun, M., Wilde, S.A., and Li, S.Z., 2005. Late Archean to Paleoproterozoic evolution of the North China Craton: key issues revisited. *Precambrian Research*, 136: 177–202.
- Zhao, G.C., Cao, L., Wilde, S.A., Sun, M., Choe W.J., and Li, S.Z., 2006. Implications based on the first SHRIMP U–Pb zircon dating on Precambrian granitoid rocks in North Korea. *Earth and Planetary Science Letters*, 251: 365–379.
- Zhao, G.C., Peter, A.C., Li, S.Z., Wilde, S.A., Sun, M., Zhang, J., He, Y.J., and Yin, C.Q., 2012. Amalgamation of the North China Craton: Key issues and discussion. *Precambrian Research*, 222–223: 55–76.
- Zhao, L., Zhang, Y.B., Yang, J.H., Han, R.Y., and Kim, J.N., 2016. Archean rocks at the southeastern margin of the Rangnim massif, northern Korean Peninsula, and their response to Paleoproterozoic tectonothermal event. *Acta Petrologica Sinica*, 32(10): 2948–2964 (in Chinese with English abstract).
- Zhu, K., Liu, Z.H., Xu, Z.Y., Wang, X.A., Cui, W.L., and Hao, Y.J., 2019. Petrogenesis and tectonic implications of two types of Liaoji granitoid in the Jiao–Liao–Ji Belt, North China Craton. *Precambrian Research*, 331: 105369. <https://doi.org/10.1016/j.precamres.2019.105369>.

#### About the first author



ZHU Kai, male, born in 1988 in Ji'an City, Jiangxi Province; doctor; graduated from Jilin University; College of Geology and Exploration Science and Technology, Jilin University. He is now interested in the study on Precambrian. Email: z1019544501k@126.com; phone: 18626644782.

#### About the corresponding author



LIU Zhenghong, male, born in 1960 in Dandong City, Liaoning Province; professor in College of the Earth Sciences, Jilin University, he is now interested in the study of structural analysis, Email: liuzh@jlu.edu.cn; Phone: 18686680810.